

# Heat-Flow-Driven Nonequilibria for Prebiotic Chemistry

Christof B. Mast\*<sup>[a]</sup>*Christof Bernhard Mast has been nominated for the special collection Systems Chemistry Talents by Board Member Ludovic Jullien.*

The origin of life, being one of the most fascinating questions in science, is increasingly addressed by interdisciplinary research. In addition to developing plausible chemical models for synthesizing the first biomolecules from prebiotic building blocks, searching for suitable and plausible non-equilibrium boundary conditions that drive such reactions is thus a central task in this endeavor. This perspective highlights the remarkably simple yet versatile scenario of heat flows in geologically plausible crack-like compartments as a habitat for prebiotic chemistry. Based on our recent findings, it is discussed how thermophoretically driven systems offer insights into solving key milestones in the origin of life research, such as the template inhibition problem, prebiotic symmetry breaking, and

the promotion of prebiotic chemistry by selective enrichment of biochemical precursors. Our results on molecular-selective thermogravitational accumulation, heat flow-induced pH gradients, and environmental cycles are put in the context of other approaches to non-equilibrium systems and prebiotic chemistry. The coupling of heat flows to chemical and physical boundary conditions thus opens up numerous future experimental research avenues, such as the extraction of phosphate from geomaterials or the integration of chemical reaction networks into thermal non-equilibrium systems, offering a promising framework for advancing the field of prebiotic chemistry.

## Introduction

The search for the processes that led to the emergence of life on early Earth is one of the fundamental questions of science and an inherently interdisciplinary endeavor. Prebiotic chemistry is central in investigating possible reaction pathways to the presumed first molecules of early life. For the reaction models under consideration, the driving non-equilibrium boundary conditions of the early Earth are critical. These are discussed in geosciences, astronomy, astrobiology, and physics, which ideally leads to an ongoing dialogue between the disciplines to constantly re-evaluate the plausibility of the considered chemistry and find more non-equilibrium systems to drive them. The interdisciplinary opening of the field in the last decades has also been accompanied by a move towards a systems approach in prebiotic chemistry, which has recently opened up new possibilities for, e.g., the joint synthesis of nucleotides and amino acids under increasingly realistic conditions,<sup>[1–3]</sup> the discovery of highly versatile, synthetic chemical replicators,<sup>[4]</sup> and the improved understanding of complex prebiotic reaction networks.<sup>[5–7]</sup>

This transition to treating more complex, higher-level systems is necessary because the emergence of a self-sustaining chemical system capable of Darwinian evolution in a fully

isolated, minimal system is impossible.<sup>[8]</sup> Just as modern life creates a wide variety of reaction conditions simultaneously through spatial heterogeneity and organization in cells<sup>[9]</sup> and can secure its existence through the supply of “simple” external energy, the raw boundary conditions on the early Earth must have led to the first selforganization of life from even simpler starting materials and nonequilibrium boundaries (Figure 1).<sup>[10]</sup> The modeling of these initial processes appears insurmountably difficult, considering the complexity of the various reaction compartments in modern life’s cells. For example, central parts of the metabolism in cells utilize complex membrane proteins that exploit chemical gradients.<sup>[11]</sup> However, the proteins themselves are synthesized elsewhere in the highly adapted reactive centers of the ribosomes.<sup>[12]</sup> Protected by membranes against dilution by diffusion or external disruptions, modern life forms transport their reactants selectively via directed processes through the cytosol,<sup>[13]</sup> which can be seen less as a disorganized “soup” and more as a highly structured functional matrix. This high degree of supply-pathway-guided structuring extends even to multicellular organisms and beyond,<sup>[14]</sup> raising the question of which processes stood at the beginning of this astonishing development. Just as living systems are driven through a constant supply of external energy,<sup>[15]</sup> there must have been external processes four billion years ago that spatially organized and fueled the initial prebiotic reaction networks that were necessary for the emergence, robust maintenance<sup>[16]</sup> and spread of the first life.<sup>[17]</sup> The search for such ideally simple non-equilibrium processes driving minimal life is not a unique feature of the Origin of Life field but also a central question of synthetic biology, where it has been successfully shown that even the simplest non-equilibrium

[a] C. B. Mast  
Systems Biophysics, Ludwig-Maximilians-University Munich, Geschwister-Scholl-Platz 1, 80539 Munich, Germany  
E-mail: christof.mast@physik.uni-muenchen.de

© 2024 The Authors. ChemSystemsChem published by Wiley-VCH GmbH. This is an open access article under the terms of the Creative Commons Attribution License, which permits use, distribution and reproduction in any medium, provided the original work is properly cited.

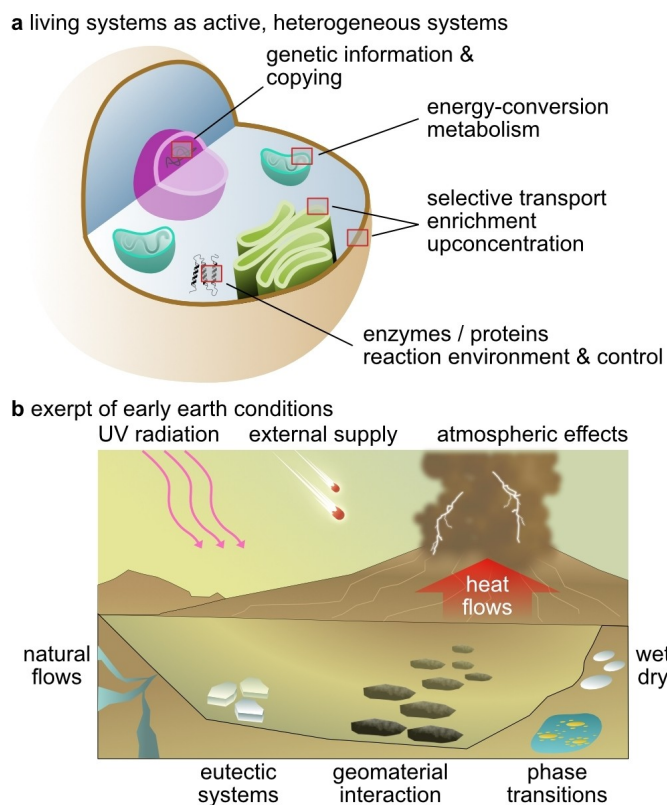


**Figure 1.** Heterogeneous systems to drive life. (a) Spatial heterogeneity in cells enables life to run an enormous number of different reaction networks in parallel in a controlled manner. Replication of genetic information, the synthesis of proteins, metabolism or the selective transport of reaction partners and products as well as their local concentration enable the maintenance of life with the supply of external energy. (b) The prebiotic earth offers a variety of different boundary conditions for prebiotic chemistry. For modelling prebiotic chemistry, it is essential to understand their interplay and how they might have implemented minimal aspects of the processes described in (a).

systems can become astonishingly life-like through spatial heterogeneity or even generate spatial selforganization.<sup>[18,19]</sup>

With this in mind, this perspective focuses on heat flows as a remarkably simple but widespread non-equilibrium process. It discusses how thermal gradients might have driven and spatially organized prebiotic chemistry.<sup>[20]</sup> First, molecule-selective thermophoresis is addressed, which is the directional movement of solutes in temperature gradients, complementing previous reviews about general non-equilibrium systems in the



Christof Mast is a physicist and senior researcher at the Ludwig-Maximilians-University Munich and has been investigating the impact of physical non-equilibrium processes on prebiotic chemistry since his PhD in 2013 and postdoc in the group of Prof Braun. Since 2018 he is Principal Investigator of the CRC235 “Emergence of Life” and CRC392 “Molecular Evolution in Prebiotic Environments”. He established a research group that investigates how heat fluxes can select, enrich and drive reactions of prebiotic substances.

context of the origin of life.<sup>[21]</sup> Then, the plausibility and availability of heat-flows on the early Earth and how these can enrich and select prebiotic molecules are covered. Moving from specific to general concepts, approaches to the problem of template inhibition in molecular evolution are addressed, concluding with the discussion of symmetry-breaking mechanisms on the early earth and the provision of optimal habitats for prebiotic molecular evolution. These aspects will be discussed with respect to previously explored models and how heat-flux driven non-equilibria compare with these existing approaches.

## Heat Flows and Thermophoresis

Heat takes on a special position in nature compared to other forms of energy. While it is represented microscopically as statistically distributed kinetic energy and thus assigns a specific temperature to an object, heat cannot be utilized in an equilibrated, closed system. As such, it is a universal energetic waste product, as it is usually produced in non-reversible physical and chemical processes according to the second law of thermodynamics until equilibrium is reached. Although it enables chemical reactions through, e.g., the heat of activation, most prebiotic models assume a thermally equilibrated system despite its ubiquitous sources on the prebiotic earth.<sup>[22]</sup> In a closed chemically equilibrated system, even catalysts would not be able to initiate any further reactions, so the question arises as to which physical non-equilibrium conditions could revitalize such inactive systems. This work aims to highlight the flow of heat as a driving force for initiating and driving chemical reactions through molecular selection and cycling of chemical conditions in a minimal space, which justifies an overview of the significant sources of heat on the early Earth or Earth-like planets (Figure 2).

Major heat sources early on are radiogenic geomaterials, primarily  $^{235}\text{Th}$ ,  $^{40}\text{K}$ , and  $^{235}\text{U}$  isotopes,<sup>[23]</sup> in the first million years also  $^{26}\text{Al}$ , which yields between  $10^6$  and  $10^2$  TW of heating power.<sup>[24]</sup> Planetary deformation by tidal forces is another heat contributor until the orbital period of the satellites is synchronized with the planet's rotation.<sup>[25]</sup> The heat generated in this way inside the planetary body can be released at the surface, for example, through volcanic activity.<sup>[26]</sup> In this process, the molten rock can be cooled quickly by contact with water, yielding an amorphous glass state,<sup>[27,28]</sup> which is under high thermal stress due to the large temperature differences that occur. The resulting interconnected and water-filled cracks in the rock can generate extensive microfluidic flow systems that implement geothermally driven flow velocities over several orders of magnitude.<sup>[29]</sup> This scenario will be discussed in more detail later. Further geological heat sources include exothermal reactions such as the serpentinization of olivine-containing rocks, which can occur continuously over thousands of years and implement porous and thermal heterogeneous hydrothermal systems.<sup>[30–32]</sup>

A heat source that is often considered to determine the habitability of a planet, e.g., the possibility of liquid water, is

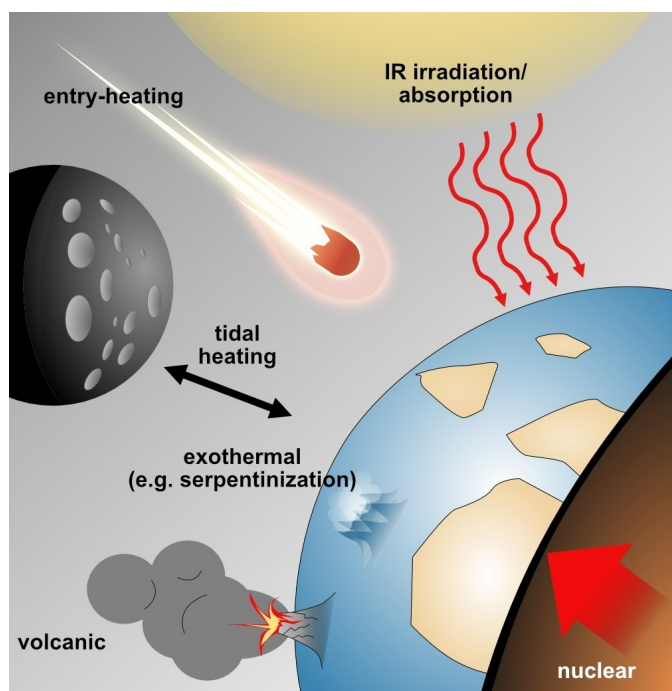


**Figure 2.** Possible sources of heat-flows on the early earth. Material heated by nuclear processes or tidal heating can reach the surface through volcanic activity, for example, and thus generate strong temperature gradients. Exothermic reactions such as serpentinization of olivine form further long-lasting sources of geothermal fluxes and heat flows. Surface temperature gradients can be provided globally by thermal radiation from the central star or locally by externally heated matter entering the atmosphere.

solar radiation and its balance between absorption and back reflection, given as albedo, that also includes the effect of prevalent greenhouse gases such as  $\text{CH}_4$ ,  $\text{CO}_2$  or water vapor.<sup>[33]</sup> Radiative heating can also cause localized temperature fluctuations due to the self-rotation of non-tidally-locked planets, thus keeping them in a constant thermal non-equilibrium to drive, e.g., continuous dry-wet cycling.<sup>[34]</sup> Even more localized sources of heat could have been implemented by the impact shock of meteorites, contributing to the synthesis of prebiotic molecules.<sup>[35,36]</sup>

In geological systems, the prevalent heat sources would lead to the formation of significant temperature gradients through the water and enclosed gas phases due to their orders of magnitude differences in thermal conductivities ( $\kappa_{\text{gas}} \sim 50 \text{ mW/mK}$ ,<sup>[37]</sup>  $\kappa_{\text{H}_2\text{O}} \sim 0.5 \text{ W/mK}$ ,<sup>[38]</sup>  $\kappa_{\text{quartz}} \sim 7 \text{ W/mK}$ ).<sup>[39]</sup> For example, fast and hot flows through rock cracks ( $T_{\text{flow}} \sim 100^\circ\text{C}$ ) that run close within 10 mm to its outer ocean-cooled wall ( $T_{\text{ocean}} = 4^\circ\text{C}$ ) could allow a temperature difference of 15 K in thin intermediate, water-filled fissures (width:  $170 \mu\text{m}$ ), which corresponds to the thermal settings often used in lab experiments.<sup>[40–43]</sup> As discussed below, even in the case where heat sources and sinks are further apart (e.g. 20 cm), temperature differences of 1 K would still be present across the  $170 \mu\text{m}$  wide pore, resulting in significant selection effects on dissolved prebiotic constituents due to the large size of geological systems.<sup>[40]</sup> Also for gases, heat conduction is still significant and strongly dependent on the geometry and

surface properties of the respective system, as it includes convective and radiative contributions in addition to diffusive conduction, making heat flows ubiquitous on the prebiotic Earth.

A direct consequence of thermal non-equilibrium systems and the resulting temperature differences, especially across liquid phases, is the driven movement of solutes, also known as thermophoresis. The directional drift  $v_T = -D_T \cdot \nabla T$  depends on the strength of the local temperature gradient  $\nabla T$  as well as on a solute-dependent thermophoretic mobility  $D_T$ . The latter has been extensively experimentally researched for systems in the Boltzmann limit of small thermal gradients  $\nabla T < (d \cdot D_T/D)^{-1}$ ,<sup>[44,45]</sup> with  $d$  denoting the size of the solute and  $D$  its ordinary diffusion coefficient, and for highly nonlinear regimes in which the time scales of thermophoretic drift become small compared to the diffusion time scales.<sup>[46]</sup> Further investigations were carried out for binary and ternary mixtures of non-polar solvents<sup>[47]</sup> and diluted solutes in aqueous solutions, especially for biopolymers such as DNA or RNA and some of their building blocks.<sup>[48–51]</sup> These experiments showed that thermophoresis, especially in aqueous media, is a surprisingly complex effect and depends on various solute and solvent properties, posing considerable challenges for its theoretical description. For colloidal particles and biopolymers, either the surface fluxes were considered as a result of heat flow-induced stresses or as a statistical system whose development can be described by a thermodynamic potential,<sup>[52–56]</sup> whereby unifying approaches were also pursued.<sup>[57]</sup> Since the thermophoretic drift will result in a local concentration gradient  $\nabla c$  of the solute, the Soret coefficient  $S_T = D_T/D$  is often used to quantify the relative strength between thermodiffusive and counteracting ordinary diffusion. In the case for prebiotically relevant molecules, e.g., charged molecules in saline, aqueous solution, the above studies show an increasing  $S_T$  with the absolute temperature  $T$ , the size of the solute  $a$ , the Debye Hückel length  $\lambda_{\text{DB}} \sim 1/\sqrt{c_{\text{salt}}}$  as a function of the salt concentration  $c_{\text{salt}}$  of the solvent, as well as the solutes surface charge  $Q_S$ . As the thermophoresis of small organic substances in aqueous solution is notoriously hard to describe theoretically, molecular dynamic simulations could make an important contribution to its understanding.<sup>[58]</sup>

Due to these complex dependencies, Soret coefficients can range in order of magnitude from  $10^{-4} \text{ 1/K}$  in the case of some salts,<sup>[59]</sup>  $10^{-3} \text{ 1/K}$  for nucleobases,<sup>[40]</sup> and up to  $1 \text{ 1/K}$  for kilobase pairs of DNA.<sup>[54]</sup> Despite these massive differences, thermophoresis itself is a weak effect. For example, the thermophoretic drift for nucleotides would be in the range of less than  $1 \mu\text{m/s}$  even for fairly steep temperature differences of  $\Delta T = 10 \text{ K}$  over  $170 \mu\text{m}$ . In equilibrium with the counteracting diffusive flux  $j_D = -\nabla c D = v_T \cdot c$ , the resulting concentration profile yields  $c(x) \sim \exp(-S_T \cdot \Delta T)$ , corresponding to a local change in concentration of only 1–2% (Figure 3a).<sup>[60]</sup> On an early Earth, such minor differences would have only a minimal influence on the prebiotic chemistry even with extreme applied temperature gradients. Given that the Soret coefficient scales inversely with the ionic strength of the solution, the high salt concentrations, often in the hundreds of millimolar regime necessary for ribozymes with magnesium salts, would lead to a

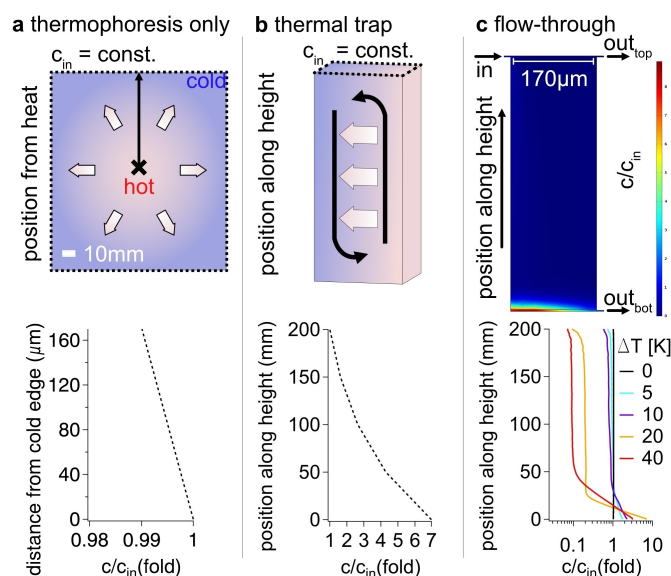


**Figure 3.** Concentration distributions in heat flow compartments. (a) A central heat source without convection leads to small concentration differences of 1–2% for nucleobases at a temperature gradient of 10 K/170  $\mu\text{m}$ . (b) The same temperature gradient including heat flow-driven solvent convection leads to two orders of magnitude higher concentration differences of nucleobases. (c) Applying a flow to the system as (b) leads to more complex concentration profiles and heat-flow dependencies.<sup>[40]</sup>

further reduction in this effect.<sup>[44,61]</sup> However, since the thermophoresis becomes stronger with the surface charge of the solute, an interesting selection possibility for phosphorylated (pre-)biomolecules arises since phosphate groups are charged under neutral conditions and could, therefore, be preferably selected by heat flows. This ability would be particularly important because phosphorus is probably scarce on the early Earth, and phosphate or phosphorylated prebiotic substances should ideally be protected from diffusion losses into the dilute bulk medium by natural processes.<sup>[62]</sup> Polyphosphates, in particular, the cyclic trimetaphosphate (TMP) are of great relevance here, as they can drive peptide formation in water<sup>[63,64]</sup> or the phosphorylation of nucleosides that boosts their Soret coefficient 2 to 3 times.<sup>[40]</sup>

Together with the theoretical models mentioned above, numerous sophisticated experimental techniques have been developed since the discovery of thermophoresis to measure its strength for various solutes. Earlier methods relied on measuring changes in electrical conductivity or potential from heat-flow-driven concentration profiles in relatively large, centimeter-scale measurement chambers to analyze the thermophoresis of salt ions.<sup>[59,65]</sup> Thanks to advances in micromanufacturing and analytical methods, measurement volumes have finally shrunk into the microliter range and below, as recently reviewed in detail.<sup>[66]</sup> Thanks to the reduced measurement volumes, even analytes that are difficult or expensive to synthesize can be investigated reliably. The main challenges using such small measurement volumes are the precise definition of the chamber geometry and temperature profile, precise temperature measurements within the heat-flow chamber, and the readout of the concentration profile generated by

thermophoresis. The temperature profiles can be generated by the absorption of IR laser beams,<sup>[48,54]</sup> by coupling heat reservoirs such as resistive heaters with highly thermally conductive materials,<sup>[67]</sup> for example, (coated) metals or sapphires if an optical readout is required, or by differently tempered flow-streams near the measurement cell.<sup>[68]</sup> In any case, continuous cooling and heating is necessary to keep the system in a thermal non-equilibrium steady state (NESS) and thus ensure a constant temperature profile.

In terms of readout, optical methods have the inherent advantage of not interfering with the concentration profile, implementing a very clean measurement system. Prominent examples include thermal diffusion forced Rayleigh scattering (TDRFS), in which a pattern is generated in the measuring chamber by the interference of “writing” laser beams, the absorption of which leads to a periodic temperature profile. The concentration and, thus, refractive index profile generated by the thermophoresis of the solute to be measured is then read out by a laser of a different wavelength.<sup>[69–72]</sup> Another method, which has been used mainly in the pharmaceutical context,<sup>[73,74]</sup> is microscale thermophoresis, in which a radial temperature profile is generated by the absorption of an IR laser spot in a capillary filled with the analyte (Figure 3a). Here, the concentration profile is measured by fluorescence microscopy, which requires prior labeling of the analytes.<sup>[75]</sup> The latter method is particularly suitable for larger biomolecules such as proteins or DNA and RNA strands, as it offers high sensitivity, nanoliter-volume capabilities, and the simultaneous measurement of several analytes when using different fluorophores. In contrast, the thermophoresis of prebiotically relevant, smaller biomolecule building blocks such as individual nucleotides, bases, or amino acids would be severely altered by the relatively large dye molecules, making non-label-based methods more suitable in this case.

The sensitivity of the above methods can be enhanced by using the principle of thermogravitational columns (Figure 3b), which is discussed in more detail below and utilized first for isotope separation in the gas phase.<sup>[76]</sup> In these cells, the different temperature-controlled sides enclose a volume with a large height-to-width ratio  $r = h/a$ , so that in addition to thermophoresis, a pronounced convection flow of the solvent is formed.<sup>[76,77]</sup> The interaction of both effects amplifies the concentration profile achieved with the same temperature difference by orders of magnitude (Figure 3b lower), which can ultimately be used to increase the signal-to-noise ratio in concentration measurements. Possible analysis methods include optical, e.g., refractometric,<sup>[78]</sup> interferometric,<sup>[71,72,79]</sup> or fluorescence-based methods,<sup>[80]</sup> but also the subsequent measurement of collected samples from spatially separate outputs in continuous flow-through systems.<sup>[41,81,82]</sup> In the context of prebiotic substances, there has recently been a need for a method that allows the concurrent measurement of thermophoresis in complex mixtures of more than 15 different compounds at low micromolar concentrations and small sample volumes. This has now been implemented by thermogravitational accumulation with subsequent freezing, cutting, and chromatographic or mass spectrometric post-analysis, yielding all analytes’ concen-

tration profiles.<sup>[40]</sup> By comparing these profiles with the results of finite element models, the relative thermophoresis of all components contained in the mixture could be determined, and predictions about the spatial separation in larger, prebiotically relevant rock-crack network systems are in reach, as discussed in later chapters. Thus, the massive amplification of the spatial separation by thermogravitational columns makes the otherwise weak thermophoresis an effect to be considered in a prebiotic scenario.<sup>[51]</sup>

## Thermogravitational Selection

Convection in thermogravitational columns not only boosts the thermophoretic accumulation of the solute to be achieved but also couples it strongly with geometry or additional drift fluxes. For the geometry, this becomes clear for the non-equilibrium steady state case, in which the concentration profile along the height  $h = r \cdot a$  of the heat flow chamber is described by:<sup>[77,80]</sup>

$$c(y) = c_0 \cdot \exp\left(\frac{\frac{q}{120} S_T \cdot \Delta T \cdot r}{1 + \frac{q^2}{10080}}\right) \quad (1)$$

with  $q = \Delta T \alpha g \rho_0 a^3 / 6 \eta D$  and the thermal volume expansion coefficient  $\alpha$ , density  $\rho_0$ , and viscosity  $\eta$  of the solvent and the local gravitational acceleration  $g$ . Figure 1 shows the result of Equation 1 in the case of  $\Delta T = 10$  K,  $S_T = 10^{-3}$  1/K, and  $a = 170$   $\mu\text{m}$  in water. In this case, the concentration  $c_0$  at the upper end of the heat flow chamber was set as constant, assuming a large reservoir or a rapid, replenishing fluid flow. The absolute achievable concentrations at the lower side of the chamber decrease accordingly in a closed chamber due to solute conservation,<sup>[42,83]</sup> which clearly shows the necessity of an open system for the prebiotic scenario. The pre-factor  $\kappa = (q/120)/(1 + q^2/10080)$  in Equation 1 has an optimum at  $q_{opt} = 0.42$ , corresponding to an optimal width  $a_{opt}$  of the heat flow chamber for a certain solute with the diffusion  $D$  and a fixed temperature difference  $\Delta T$ <sup>[77,84,85]</sup> and thus to a selection pressure to prebiotic compounds, which is not present in the case of "pure" thermophoresis without convection. While the final accumulation in the equilibrium case of Equation 1 increases exponentially with  $S_T$  and the aspect ratio  $r$ , this applies only approximately to the scaling with  $\Delta T$ .

In the  $q$ -dependent limiting case of large temperature differences, no additional accumulation is achieved due to the significantly interfering faster convection. At the same time, at very small  $\Delta T$ , only a sub-exponential dependency is expected. This somewhat unintuitive behavior is even more prominent in experimental systems since the steady state from Equation 1 is usually not reached during the experiment. Typical relaxation times for the accumulation process were estimated in<sup>[77]</sup> to  $\Phi \sim a^2 r^2 / (\pi^2 D) \cdot (1/q^2/7680)$ , usually increasing parabolically with the size of the system and solute, and reaching orders of magnitude of weeks or months, especially in larger thermogravitational columns ( $r > 100$ ) with polymeric solutes ( $D < 100 \cdot 10^{-12} \text{m}^2/\text{s}$ ).<sup>[42,86]</sup> In this case, the dependencies shown

in Equation 1 are not directly applicable but must be explicitly determined numerically for more complex experimental systems by, e.g., finite element methods. This is particularly evident in the open systems relevant to the prebiotic context, as illustrated in Figure 3c (adapted<sup>[40]</sup>). Here, a heat flow chamber is continuously filled by an inflow at the top of the chamber and emptied at the opposite top and bottom at the same flow rate, resulting in a non-exponential concentration distribution even in the stationary case due to the perturbative flow-through.<sup>[41]</sup> The above considerations illustrate that, despite the simplicity of the boundary conditions, thermogravitational accumulation exhibits an astonishing variety of selection opportunities, especially for the smaller prebiotic reaction products, whose Soret coefficients can differ by orders of magnitude.<sup>[40]</sup> Thermogravitational accumulation was further shown to be robust even against large temporal fluctuations of the applied temperature gradient<sup>[40,43]</sup> or geometry irregularities<sup>[80]</sup> and, as Equation 1 shows, has no threshold values in  $S_T$ ,  $r$  or  $\Delta T$  below which the effect breaks down, making it a plausible non-equilibrium process on the early Earth.

In the systems of interconnected rock cracks introduced above, e.g., thermally stressed basalt glass, a natural implementation of a microfluidic network of heat flow chambers covering a wide range of flow and boundary conditions would, thus, form a complex prebiotic selection machine.<sup>[40,87,88]</sup> Recent studies showed that this heat-flow-driven, selective accumulation also couples to various chemical processes and thus generates higher-order effects relevant to prebiotic chemistry. For instance, due to the charge-dependent Soret coefficient, proton donors and acceptors are differently accumulated in buffers or acid-base reaction systems and depleted at the upper end of the heat flow chamber, respectively. This imbalance creates pH gradients of up to 9 units along the height of the chamber.<sup>[41,80]</sup> While this would not be expected due to the high diffusion rate of the hydronium ion<sup>[89]</sup> and thus rapid pH equalization, local charge neutrality and the strong thermophoresis of the, e.g., buffer compounds stabilize the pH differences even along these small millimeter scales. Since the pH in turn strongly influences the charge or binding state as well as the stability of prebiotic compounds such as RNA, it can be assumed that heat-flow-driven pH gradients are able to directly impact the course of prebiotic reactions. As simple salts also undergo thermophoresis,<sup>[59]</sup> the local ionic strength is also strongly influenced by the heat flow-driven accumulation effect, which could alter the stability of fatty acid vesicles or enable the correct folding of ribozymes. Due to the dependence of thermophoresis on the ionic strength and pH-determined charge state of the solute, these systems are highly coupled, which makes modeling difficult, but also implies an extremely rich selection system for the prebiotic scenario.

## Heat Flow-Driven Approaches to the Origin of Life

Thermal non-equilibrium systems can, therefore, selectively spatially arrange prebiotic substances and adjust their chemical boundary conditions. While this is a long way behind the ability of modern life to generate local reaction niches and optimal conditions for self-preservation, it raises the question of how thermal non-equilibria could facilitate particular key steps in prebiotic chemistry and how they could contribute to driving cyclic reaction networks as a critical property of living processes.<sup>[8,90]</sup> In the following section, not only specific problems of the RNA world, such as template inhibition, will be considered, but also more general challenges on the way to the first living systems, such as the concentration problem or the driving of complex reaction pathways without the exploding number of detrimental intermediates.<sup>[91]</sup>

### Approaches to the Strand Inhibition Problem

One often considered model for emergent prebiotic systems is the RNA world,<sup>[92–95]</sup> in which RNA acts as a catalyst as well as a genetic information store, thus eliminating an otherwise occurring chicken-and-egg problem between proteins and the genetic memory that encodes and is copied by them.<sup>[96]</sup> The RNA world concept has been extensively researched over the last decades.<sup>[97–100]</sup> It includes as central milestones the synthesis of RNA building blocks from prebiotically plausible components, the de novo polymerization of oligonucleotides, and their nonenzymatic replication, from which the first ribozymes emerge through molecular evolution. Directed evolution has already led to the discovery of a large number of such ribozymes, such as the sunY,<sup>[101]</sup> R3 C,<sup>[102]</sup> or class I ligase.<sup>[103]</sup> The latter served as the basis for the directed evolution of advanced RNA-polymerases, which enabled base-by-base copying of ever longer,<sup>[104]</sup> more complex,<sup>[99]</sup> and cross-chiral templates,<sup>[105]</sup> even utilizing non-canonical nucleotides.<sup>[106]</sup> In this context, it is assumed that the nonenzymatic copying of RNA polymers required for the molecular evolution of the first ribozymes must have already succeeded, albeit much more slowly, but still with sufficiently high fidelity so that the resulting gene pools were not lost due to the error catastrophe.<sup>[107]</sup> Nonenzymatic replication of RNA was achieved in the lab by prior activation of the nucleotides<sup>[108,109]</sup> in a base-by-base and in a ligation replication scheme.<sup>[110,111]</sup> While highly evolved enzymes exhibit error correction mechanisms and thus ensure high fidelity in replication, it has been shown that a similar error correction effect could be implemented in such prebiotic, nonenzymatic copying processes by stalling upon incorporation of non-matching nucleotides.<sup>[112,113]</sup>

Both enzymatic and nonenzymatic replication suffer from the central problem of template inhibition (Figure 4a). As soon as the product strand has been successfully extended, it must be removed from the template to restart the process on both strands. If this is not achieved, replication stalls or only parabolic

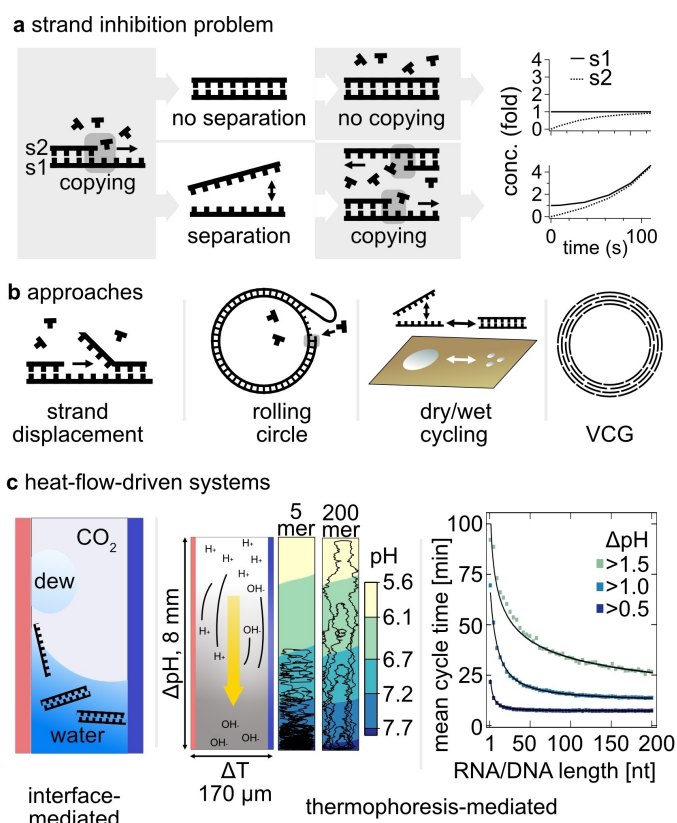


**Figure 4.** Approaches to the strand inhibition problem: (a) Unless the product is removed from the template, replication halts after the reverse complement is created. (b) Product separation may occur through invading strands, fuel-driven, catalytic rolling-circle replication, or by varying the product or salt concentration through dry-wet cycles. High product affinities can be avoided by e.g. a virtual circular genome model (VCG), in which only shorter, overlapping partial elements of the entire genome have to be replicated. (c) Heat flows allow the local cycling of pH, temperature as well as salt and substrate concentration at CO<sub>2</sub>-gas interfaces or through the thermophoretic generation of pH gradients.<sup>[80]</sup>

growth is possible,<sup>[114]</sup> which can prevent the selection of the fittest species and thus represents a major obstacle to molecular Darwinian evolution.<sup>[115]</sup> The inhibition of the template can occur either due to the strong binding energy of the formed product-template complex or, often the case in closed systems, due to the high product concentration present in the later course of replication, leading to a rapid reannealing of the product even after its intermediate dissociation. The limiting product concentrations depend on the speed of the replication reaction and can therefore be in the nanomolar range for nonenzymatic RNA-based schemes.<sup>[116]</sup> Ribozyme based systems with high required Magnesium concentrations also suffer from hydrolysis at elevated temperatures that are often applied periodically to dissociate the product,<sup>[61,117]</sup> similar to polymerase chain reactions.<sup>[118]</sup> Activated RNA nucleotides that feed copying reactions are also often affected by hydrolysis, so they, e.g., have to be removed and replenished by washing steps after immobilization of the product strands to allow further replication cycles.<sup>[119]</sup> An exchange of the no longer active nucleotides by high, often millimolar concentrations of activated nucleotides with simultaneous retention of the products

could have been facilitated, for example, by fatty acid protocells, which are permeable for the small feeding molecules, but not for larger (RNA) polymers.<sup>[120]</sup>

In such systems, the high required reactant concentrations for these reactions could have been generated by dry-wet cycles<sup>[121,122]</sup> or by the formation of eutectic phases, in which the phase transition of the water into the ice phase leaves strongly concentrated salts and building blocks in the solution at a reduced freezing point.<sup>[104,123]</sup> At the same time, the low temperatures prevailing here would primarily suppress the hydrolysis of the RNA, while the millimolar magnesium concentrations would enable efficient replication by ribozymes.<sup>[104,123]</sup> While template inhibition still poses a problem in such systems without further cycling of the environmental conditions, it could be circumvented in de-novo synthesized, self-assembled chemical replicators. Here, the replicator assemblies broke apart independently after reaching a certain size, whereby each of the fragments could serve as a new template for further replication cycles.<sup>[4]</sup>

For RNA systems on the other side, strand displacement<sup>[124]</sup> offers a way to remove blocking oligonucleotides by the invasion of short RNA strands using a branch migration mechanism, which allows further primer extension by activated nucleotides (Figure 4b).<sup>[125]</sup> However, it has been argued that in the case of linear templates, it is unlikely that a complete copying process can be carried out using toehold-mediated strand displacement, as the short invading primers themselves are displaced too quickly by the old product in a reverse process.<sup>[116]</sup> This problem would be avoided for circular templates, as the extending product would displace itself after one replication cycle. Here, the reverse displacement by the dissociated part of the product would be circumvented by its constant cleavage, e.g., by a self-cleaving ribozyme or hydrolysis.<sup>[116]</sup> This approach was also addressed experimentally in a ribozyme-catalyzed rolling-circle replication, in which triphosphate trinucleotides were used as building blocks. It resulted in longer products than the original template, demonstrating successful strand displacement.<sup>[126]</sup> However, a challenge in this approach is the simultaneous need for circularizing and cleavage ribozymes to complete the replication cycle and exceed linear growth.

Primer-initialized RNA replication also adds the difficulty to find matching primer sequences for each template from the start, as these are considered sparse in the vast initial pools of strands with random sequences. Since the templates must be copied down to the last base to enable reverse primer binding, being a notoriously unreliable step, a virtual genome model was recently introduced to circumvent these problems.<sup>[127]</sup> Instead of a single large template strand and the associated strongly binding product strand, the prebiotic genome is assumed to be fragmented, with the individual fragments overlapping and thus representing a virtual circular genome. Here, possible advantages are the simpler strand displacement due to the shorter length of the particular strands and the ability of each fragment to serve as a primer for a copying process. Recent experimental tests show successful primer extension in such a setting but point to the need for environ-

mental fluctuations of salt concentration, hydration state, pH, and the feeding of building blocks to enable uniform product dissociation and reattachment of the genome fragments for a further replication step.<sup>[128]</sup>

Dry-wet cycling and fluctuation of substrate and salt concentration could have been implemented on the surface of early earth on a relatively large scale by tidal or daily cycles or by surface wetting, e.g., rain or geysers<sup>[129,130]</sup> to facilitate de-novo RNA polymerization.<sup>[83,122]</sup> However, the separation of product and template necessary for successfully copying RNA with simultaneous prevention of immediate reannealing is challenging via pure concentration fluctuations since RNA's melting temperature for strands of approximately thirty base pairs or more was considered practically impossible under prebiotic conditions due to its melting temperatures exceeding the boiling point of water.<sup>[131]</sup>

Studies that rely on temperature fluctuations for strand separation only, therefore, require additional compounds in the case of RNA to reduce its melting temperature,<sup>[132]</sup> use short templates,<sup>[133]</sup> or switch to DNA templates and protein polymerases as a proxy system<sup>[134,135]</sup> but are by definition applicable in thermal non-equilibrium systems with its features discussed above. The product of the replication reaction can thus be protected from diffusive dilution by its thermophoretic accumulation.<sup>[134]</sup> If such a system is open and fed with a continuous inflow of fresh building blocks, only products with a large Soret coefficient, such as long nucleotide polymers, can remain in the system permanently and be replicated while short products are flushed out. The latter system would be protected from forming short parasitic strands, which could be replicated faster but would lose important genetic information of the original template,<sup>[135]</sup> often referred to as Spiegelman's monster.<sup>[136]</sup> The selection pressure is not limited to the template size – any process that would penalize one strand or sequence over the other would quickly lead to its extinction, offering exciting possibilities to implement complex, Darwinian evolving systems. However, such systems based on thermal cycles alone can do little for enzyme-free copying due to the mentioned high melting temperatures required for RNA and the resulting greater hydrolysis, which can take up to weeks for a copying process.<sup>[137]</sup>

Efficient detachment of the product from the template occurs ideally in conjunction with a reduction in the local salt concentration and a reduction in the pH value.<sup>[21,138]</sup> The latter, in particular, was proposed to reduce the melting temperature of, e.g., 13mer RNA from 66 °C at pH 7.1 to 13 °C at pH 3.6 and thus even enable separation without additional temperature oscillation.<sup>[139]</sup> While oscillations of the pH value can be problematic in bulk systems, as the sequential addition of acids and bases greatly increases the salt content of the solution, non-equilibrium systems offer interesting possibilities here: As discussed above, thermal non-equilibria not only generate temperature oscillations but can also couple the chemical boundary conditions of the reaction solution. For example, a temperature difference at a CO<sub>2</sub>-gas-water interface forms a chemically surprisingly heterogeneous system in a confined space.<sup>[140,141]</sup> On the warm side, water is evaporated from a DNA-

replicating solution and condenses on the cold side as droplets, saturates with CO<sub>2</sub> and thus acidifies. If this acidic drop of water falls back into the reaction solution, it briefly creates a region with low salt content and low pH, ideal for separating template-product complexes (Figure 4c, left). Under such conditions, DNA evolution to sequences with a melting temperature corresponding to pH and salt conditions was demonstrated in a PCR reaction<sup>[141]</sup> and a SunY-ribozyme-catalyzed ligation.<sup>[142]</sup> In the latter RNA scenario, the hydrolysis problem described above plays a significant role due to the slow ribozyme activity, but it also competes with the reannealing of already formed products.<sup>[116,131]</sup> Both challenges could be addressed in a liquid-phase-only, thermophoretic accumulation system.

We were able to show that the heat-flow driven pH gradients of up to 9 units over the entire chamber height not only depend on the geometry and the applied temperature difference,<sup>[80]</sup> but can be tuned and controlled over a wide pH range by the composition of an acid-base reaction system.<sup>[41]</sup> While characterization of heat-flow driven pH gradients for other reaction systems is still to be done, an ideal condition for RNA-based replication reactions could be created by implementing low, hydrolysis-suppressing pH conditions (5) in the lower part of the chamber and neutral-slightly-alkaline conditions in the upper part of the chamber: At the bottom, the reaction product would be protected from hydrolysis and dilution and stored as a single strand due to the low pH. Since the thermophoretic generation of the concentration profile is a stochastic effect, the long RNA strands would by chance enter an upward convection stream by local diffusion, in which they can anneal with smaller and therefore less well localized primer strands as the pH increases and finally ligate under optimal reaction conditions before being stably stored again in the lower chamber area. As the concentration of the long product strands in the upper chamber area would be greatly reduced, product reannealing to the template could thus be effectively prevented (Figure 4c, right). The usual cycle times of such vertical, convection-driven pH gradients ( $\Delta pH \sim 1.5$ ) for DNA or RNA in, e.g., phosphate buffer systems, are, depending on their length, in the range of approx. 20 minutes to a few hours for chambers (8 mm height, 0.17 mm width) with an applied temperature difference of 14 K. This leads to residence times in the range of 5–10 minutes in the upper/low-pH chamber environment, especially for longer polynucleotides (Figure 4c).<sup>[80]</sup> Similar cycle times would also apply to the formic-acid-based, heat flow-driven pH gradients.<sup>[41]</sup> The applications of this system could extend to the pH cycling of protocells,<sup>[143,144]</sup> which would thus generate a constant pH gradient across their membrane and could be used as a protonmotive force. Thus, pH-heterogeneous systems generated in this way would support RNA-based systems, but also make a general contribution to prebiotic reaction pathways that require varying pH conditions.

## Heat Flows as a Tool for Prebiotic Sequence Selection

Just as other non-equilibrium processes, heat flows can push systems out of an initially symmetric equilibrium, therefore breaking the symmetry of a variety of prebiotically relevant parameters. The first obvious example of this is the concentration profile itself, described by Equation 1 as the result of compound-selective thermogravitational accumulation from homogeneous initial conditions (Figure 5c right).<sup>[43]</sup> Symmetry breaking in the sequence space of oligomer pools and chiral symmetry breaking are further examples considered to be essential in the prebiotic context (Figure 5a).

The former describes the transition from naïve sequence pools in which each sequence occurs with equal probability to weighted pools in which certain groups of sequences and corresponding folds occur particularly frequently. Sequence biases could be caused by the preferential copying of specific sequences or filter mechanisms, e.g., by interaction with

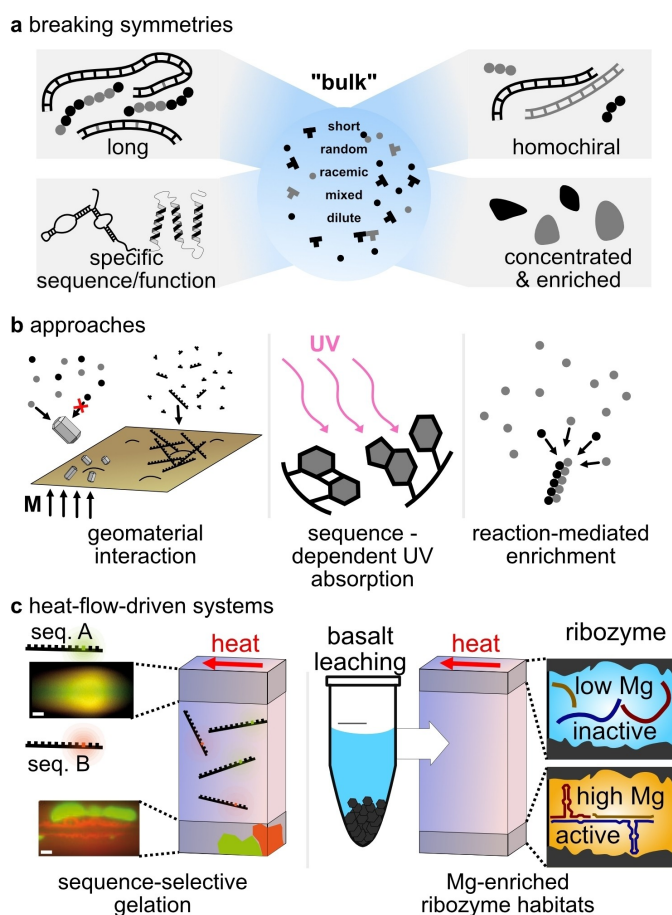


**Figure 5.** Symmetry breaking as a prerequisite for the emergence of life. (a) Examples of symmetry breaking from homogeneous, dilute and random mixtures to homochiral, longer, functional polymers and enriched concentration spots. (b) Interaction with mineral surfaces and radiation as well as reaction-mediated enrichment can introduce biases in initially homogeneously distributed pools of different sequences and compositions. (c) Self-enhancing thermogravitational accumulation can lead to sol-gel phase transitions and the formation of sequence-pure gels. Scalebars (white) correspond to 20  $\mu\text{m}$ .<sup>[152]</sup> The selective enrichment of divalent salts such as magnesium from the leaching equilibrium with basalt enables the function of ribozymes.<sup>[43]</sup>



minerals or other solutes that can withhold specific sequences from random pools. If such a process favored particularly compactly folding RNA strands, this could increase the probability of obtaining functional RNA or ribozymes in the resulting pool.<sup>[145]</sup> For example, ribozyme polymerases with a length of over 100 nucleotides could thus be found more quickly in contrast to a brute-force search of the complete sequence space with a size of  $4^{100} \sim 1.6 \cdot 10^{60}$  sequences, which is practically impossible. The formation of long RNA polymers thus inherently breaks the symmetry in sequence pools since not all sequences can occur in them for combinatorial reasons alone.

The latter, chiral symmetry breaking, describes the transition from initially racemic mixtures, in which the enantiomers of a species occur with equal probability, to mixtures with enantiomeric excess, i.e., the dominant occurrence of one of the enantiomers.<sup>[146–148]</sup> Since the biopolymers occurring in nature, such as DNA, RNA, and polypeptides or proteins, are homochiral, understanding their formation from racemic building-block mixtures is central to answering the emergence of life problem.

These symmetry-broken states discussed above are difficult to achieve, unlike the self-establishing equilibrium states that are usually symmetric in concentration or composition. A well-known example of such a difficulty is called Spiegelman's monster, which describes the tendency of replicators to favor simpler and shorter substrates, as these can be replicated remarkably quickly.<sup>[136]</sup>

For example, long ribozyme polymerases have difficulty replicating equally long RNA polymers, leading to a preference for shorter RNA templates.<sup>[132,149]</sup> Combined with the known chemical instability of RNA in water, where the probability of strand breakage by hydrolysis increases exponentially with its length,<sup>[117]</sup> this demonstrates the information-need paradox in the origin of life that states the difficulty of replicating information-rich and long polymers.<sup>[150]</sup> A solution has been proposed in synthetic chemical replicators, in which more complex molecules would be chemically more stable than shorter ones.<sup>[4]</sup> Concerning RNA, this is partly already the case as it fragments slower by hydrolysis in Watson-Crick base-paired complexes,<sup>[117,151]</sup> favoring longer sequences with a higher G/C base content.

However, this property does not solve the preference for simple parasitic strands in replication processes. Therefore, selective mechanisms that favor functional or more complex replicates are necessary to avoid falling back to the simplest possible system, which would otherwise inhibit molecular evolution. It has already been shown that transient compartmentalization of ribozymes coupled with a selection of their function can prevent parasitic strands from taking over.<sup>[153]</sup> In a natural context, many possible selection mechanisms were proposed. For example, length-dependent selection by adsorption on mineral surfaces was demonstrated<sup>[154]</sup> (Figure 5b), which, however, imposes additional conditions on selectable ribozymes by influencing the possible folding states of the RNA bound.<sup>[155]</sup> It was also shown that the mutual binding ability of such binding oligonucleotides leads to a selection of sequence

patterns through their complex formation and sedimentation from a larger pool in an open system.<sup>[156]</sup> Furthermore, potentially prebiotically plausible, simple peptides could self-aggregate into amyloids and the resulting cross-beta structures into functional units<sup>[157,158]</sup> if selected and concentrated from dilute prebiotic ponds. Phase separation of RNA and simple peptides into coacervates, which have been investigated as a promising approach for prebiotic compartmentalization,<sup>[159,160]</sup> also offers selective uptake of RNA with specific sequence motifs,<sup>[161]</sup> suggesting exciting additional selection pressures for RNA replication. Such liquid-liquid phase separating systems are particularly interesting because ribozymes operating in them change the physical properties of the coacervate droplets and, thus, potentially also their aforementioned selective properties.<sup>[162]</sup>

Further external selection pressures on a prebiotic earth would be the interaction with incoming radiation, e.g., in the UV range. Self-folding oligonucleotides would have lower absorption of UV photons through the formation of Watson-Crick base pairs and, thus, a potential selection advantage over non-folding strands.<sup>[163]</sup> This would give longer replicated template-product complexes an advantage over smaller replication complexes, which can separate more easily from UV-prone single strands due to their lower melting temperature. Since UV damage is specific to certain bases or base sequences, this would additionally result in an implicit sequence selectivity, the influence of which must be taken into account in surficial models.<sup>[164,165]</sup> Non-destructive selection schemes of longer oligomers would be particularly interesting for RNA-copy models such as the Virtual Circular Genome, since in a pool of short oligomers and building blocks, the resulting superimposed u-shaped length distribution would lead to a higher copy rate, as recently shown.<sup>[128]</sup>

While some of the chemical and physical selection mechanisms discussed above inherently favor specific sequence patterns or strands with a biased base content, the various polymerization and replication schemes themselves can also introduce sequence and length biases into prebiotic pools. For example, it was shown that RNA polymerization from Nucleoside 2',3'-cyclic phosphates generates product pools with a G-bias,<sup>[83]</sup> while also enzymatic RNA copying using ribozyme polymerases is prone to show strong sequence preferences.<sup>[166]</sup> Such biases could be prevented by using cross-chiral ribozymes that avoid strong sequence-specific interaction between enzyme and substrate.<sup>[105]</sup> Ligation processes already mentioned above can also implement a replication system for short templates if the even shorter substrates are sufficiently replenished by upstream polymerization reactions. Here it was shown that sequence symmetry can be broken, and structured sequences can emerge dominantly from a random sequence pool.<sup>[167,168]</sup>

Interestingly, accumulation in thermogravitational columns also enables symmetry breaking in the sequence space of oligomers. Since these columns select molecules depending on their charge and size, among other things, feedback cycles with elongation reactions, such as the splint-like linkages of short substrate strands by Watson-Crick base pairing, can emerge.

Here, the size of the resulting complexes is governed by the concentration of the substrate. Due to the efficient accumulation of long strands in thermogravitational columns, the total substrate concentration is also greatly increased, leading to ever larger complexes and substrate concentrations.<sup>[42]</sup> The length distribution of the complexes also depends on the binding energy of the substrates to each other. While a singular sequence modification in bulk only leads to a minimal change in the length distribution, such differences are amplified by the heat-flow-driven feedback cycle. For hydro-gel-forming DNA, it could be shown that this effect even distinguishes single-point mutations and can generate locally separate, sequence-pure oligonucleotide gels (Figure 5c).<sup>[152]</sup> While mutually binding strands would be selected in such processes, it was shown that also individual bases and nucleotides exhibit significantly different thermophoresis. T, C and U could thus be enriched up 32% against G and A in a heat flow chamber implementing a temperature gradient of 15 K over 170  $\mu\text{m}$  width after 18 h.<sup>[40,48]</sup> In combination with a polymerization reaction such as that of the Nucleoside 2',3'-cyclic phosphates mentioned above, the G-bias of the polymerization could be compensated by a G-depleting thermogravitational accumulation and thus generate a more balanced sequence pool. In contrast, replication reactions with a DNA proxy system triggered by heat flows at CO<sub>2</sub>-gas-water surfaces were shown to generate not only very long but also sequence-divergent product strands through probably unspecific sequence interactions at the interface. The drift towards A/T-rich sequences compensated for the increasing length, thus maintaining a relatively low melting temperature that ensures product separation and the successful continuation of the replication reaction.<sup>[141]</sup>

In summary, this shows the importance of including length and sequence selection by external mechanisms and the possible sequence bias by the prebiotic chemistry itself. Resulting product pools could, for example, be examined regarding their ability to self-fold into functional structures, which would significantly facilitate the autonomous selection of the first ribozymes compared to a completely naïve sequence pool.<sup>[145]</sup>

### Non-Equilibrium Enrichment of Homochiral Compounds

Also, with regard to the above-mentioned symmetry breaking towards homochiral polymers, as required for the formation of functional folding structures and interactions of biopolymers, major progress has recently been made in the investigation of external non-equilibrium systems as previously reviewed.<sup>[169,170]</sup> A well-known example is the asymmetric autocatalysis of small molecules in the Soai reaction, in which an initial small enantiomeric excess is boosted due to enantioselective catalysis driven by a chemical non-equilibrium.<sup>[171]</sup> The synthesis of homochiral ribo-amino-oxazoline, an RNA precursor, was further achieved by the enantiopure crystallization that started from an initial enantiomeric excess of only 1%.<sup>[172]</sup> Such enantiopure crystallization has also been shown to interact with natural magnetites through chiral-induced spin selectivity, leading to

their avalanche-like magnetization and, thus, to self-enhancing feedback.<sup>[173,174]</sup> For the synthetic, self-assembled chemical replicators mentioned above, it was further shown that these can also self-assemble enantiopure from racemic mixtures. They thus offer a unique model system that inherently overcomes a number of important core problems for emergent life, even though they are chemically unrelated to the canonical biopolymers.<sup>[175]</sup> However, it has been hypothesized that homochirality is an inherent property of larger molecules containing more than 10 atoms of the same or higher mass than carbon that are part of large nonequilibrium reaction networks.<sup>[176]</sup>

Could thermal non-equilibrium systems also contribute to the selection of homochiral biopolymers or their precursors? Recent results on the thermogravitational accumulation of L- and D- amino acids such as cysteine, threonine or serine, for example, show no selective effect between the enantiomers, which was to be expected in an achiral solvent such as water and without high concentrations of other chiral species.<sup>[40]</sup> Indirectly, however, heat flows could certainly play a role locally. For example, RNA precursor crystals could be grown through heat-flow driven dry-wet cycles driven at gas-water interfaces, which indicates that this process can also be used for their enantiopure enrichment.<sup>[177,178]</sup> Another indirect mechanism driven by heat flow could take advantage of the fact that otherwise chiral oligonucleotides can no longer successfully form Watson-Crick base pairs with even just a few incorporated L-nucleotides.<sup>[179]</sup> Together with the sequence-dependent hydrogelation of oligonucleotides described above, a small number of contained L-nucleotides instead of small sequence differences would now be sufficient to prevent thermogravitational amplified hydrogelation. In a pool of G/C-rich and interacting strands, homochiral strands could thus be reliably filtered out and protected from diluting diffusion by heat flows.<sup>[54,152]</sup>

### Heat Flows to Set a Molecular Kitchen for Prebiotic Chemistry

While the heat flow approaches to template inhibition and symmetry breaking were discussed above mainly regarding an information-centered approach to the origin of life, i.e., the RNA world, more general applicable features of thermal non-equilibrium systems will now be addressed. A key "benchmark" feature of prebiotic reaction pathways is their one-potability under early-earth conditions,<sup>[180]</sup> i.e., their capability to obtain high yields of the desired product in a single reaction compartment without external intervention. Together with the prebiotic availability of the starting materials from geological sources or meteorites, this characterizes the plausibility of prebiotic models.

However, approaches with only a few simple prebiotic compounds that are considered plausible, such as the aminonitrile synthesis in the Miller Urey type electrical discharge experiments<sup>[181]</sup> or the synthesis of sugars in the formose reaction, often lead to a confusing variety of undesirable by-products, prebiotic clutter,<sup>[91]</sup> or arbitrary complexation to tar-

like molecules.<sup>[182]</sup> To address this challenge, an increasing range of prebiotic biomolecule synthesis pathways have recently been implemented in one-pot experiments, such as nonenzymatic nucleobase synthesis,<sup>[183]</sup> DNA nucleoside synthesis,<sup>[184]</sup> or glycoside synthesis.<sup>[185]</sup> Furthermore, peptide synthesis with the aid of RNA toward early translation was shown, which, however, requires stepwise adjustments of pH and temperature.<sup>[98]</sup> To prevent undesirable side reactions, these reactions must also be initiated with as pure starting materials as possible, which are probably difficult to obtain in prebiotic systems. Intermediate laboratory steps, e.g., for the complex, synergistic synthesis of RNA, protein, and lipid precursors<sup>[11]</sup> or of activated nucleotides<sup>[186]</sup> were shown to be compatible with uninterrupted flow chemistry. Convergent flow models have also been proposed for unified purine and pyrimidine ribonucleotide synthesis, thus making the usual laboratory reaction steps plausible in a prebiotic environment (Figure 6 a/b).<sup>[187]</sup>

In order to keep this combinatorial explosion of the unwanted and low yields of the desired products in check, non-equilibrium systems that trigger selective processes were discussed, such as the discussed dry-wet cycles that enable

selective crystallization of intermediate products for synthesizing nucleosides from prebiotically plausible building blocks.<sup>[188]</sup> It was shown that goethite mineral surfaces or membranes could potentially enhance conditions for, e.g., the synthesis of aspartate dimers.<sup>[189]</sup> Also, the carbohydrate synthesis<sup>[190]</sup> and the oligomerization of pyrophosphates<sup>[191]</sup> were demonstrated experimentally on montmorillonite, opening a way to guide the prebiotic chemistry to produce the desired products in higher yield. Said condensation reactions leading to ribo-oligonucleotides and peptides are particularly challenging without condensing agents due to their release of water in an aqueous medium, which describes the so-called “water problem”.<sup>[192]</sup> This results in the paradox that although water is essential for the development of life, it also hydrolyzes its basic building blocks, especially RNA.<sup>[150]</sup> With the right timing, i.e., not too long destructive wet times,<sup>[43]</sup> the above-mentioned dry-wet cycles have been identified as a possible approach to this issue. For example, the primer extension<sup>[83,122]</sup> or RNA polymerization<sup>[121]</sup> discussed above regarding the template inhibition problem was achieved using such cycles. Other examples include the dry-wet-cycle-driven oligomerization of proteinogenic amino acids<sup>[193,194]</sup> or the mutual stabilization of RNA and proto-peptides.<sup>[195,196]</sup> Relaxing the requirements for the environmental boundary conditions of dry-wet cycles, it was also shown that the condensation to N-acetyl peptides by chemo-selective aminonitrile coupling could take place with the help of prebiotically plausible hydrogen sulfide thioacetate and ferricyanide even without the intermediate removal of water.<sup>[192]</sup> Remarkably, this reaction can proceed completely in one pot without purifying intermediates, given a well-defined starting mixture.

While the above examples show that important parts of prebiotic synthesis are indeed possible under homogeneously well-mixed, one-pot conditions, it is also apparent that the overarching development from the first starting materials to a Darwinian molecularly evolving system requires very different, even periodically changing boundary conditions and an open system in the respective stages. The possibility of symmetry breaking of local concentration equilibria by heat flows through connected cracks of rock offers interesting possibilities for implementing various chemical initial conditions in a volumetrically scaling system. While dry-wet cycles in individual heat flow chambers on enclosed gas bubbles could implement many of the effects driven by surface-bound dry-wet cycles,<sup>[177]</sup> this setting offers additional benefits. For example, the cycle periodicity in these thermal gradient systems depends significantly on the strength of the applied heat flow and the chamber geometry<sup>[140,141]</sup> and is thus decoupled from fixed tidal or diurnal cycle times. Due to the large extent of such geological fissure systems, a large number of different settings could be explored in separately existing fissures simultaneously and thus be home to prebiotic chemistry incorporating a wide variety of reaction rates.

In liquid-only systems where gas-water interfaces and the corresponding Marangoni-flows are not disturbing local convection fluxes,<sup>[197]</sup> the enrichment of different prebiotic solutes by selective thermogravitational up-concentration becomes

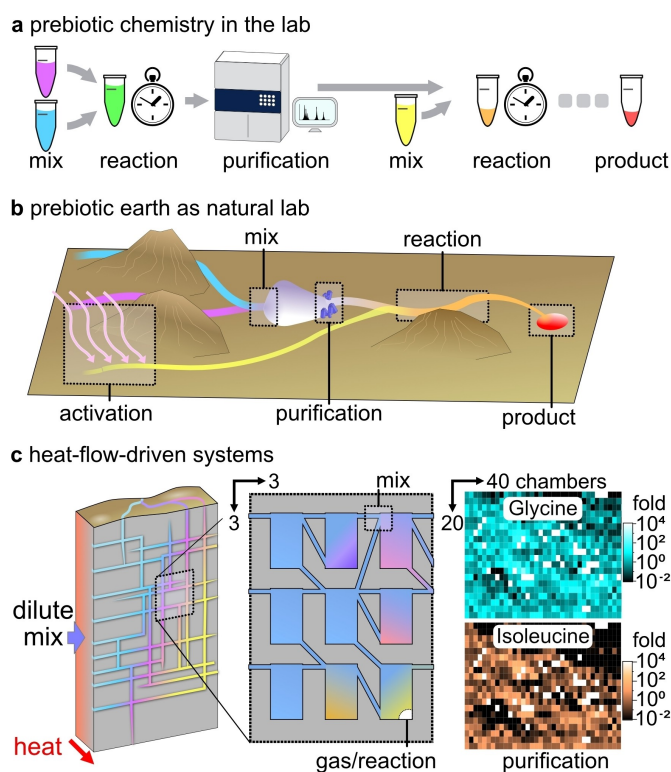


**Figure 6.** (a) Prebiotic synthesis often requires several intermediate steps in which products are purified or in which new substrate must be added in a defined manner. (b) Such reaction steps from the laboratory can be implemented on early Earth by a favorable sequence of converging water streams (mixing) or slightly drying water points (concentration). (c) In randomly connected rock fissures through which a slow geothermal flow is driven, heat flows could have spatially separated the solutes contained therein and mixed them together again in a defined manner, thus implementing a prebiotic macro-lab. The right panels show glycine (upper) and isoleucine (lower) concentrations relative to their initial concentrations in a system of 20 x 40 randomly connected chambers (200x60x0.17 mm each), ranging between  $c_{G,min} = 2 \cdot 10^{-4}$  and  $c_{G,max} = 490$  ( $\bar{c}_G = 5.4$ ) and  $c_{I,min} \sim 1 \cdot 10^{-12}$  and  $c_{I,max} = 1122$  ( $\bar{c}_I = 7.8$ ), respectively.<sup>[40]</sup>

predominant. Initially shown for sodium-rich basalt leachates,<sup>[43]</sup> yielding optimal conditions for the function of ribozymes by thermogravitational enrichment of magnesium, it has recently been demonstrated that more complex mixtures of prebiotic compounds can also be selectively enriched in such connected, heat flow-driven crack-systems (Figure 6c).<sup>[40]</sup> Based on experimental results from one or three interconnected chambers, it was possible to show in a numerical model of 20 by 20 connected compartments that the concentration ratios between different amino acids can be shifted by up to 3 orders of magnitude in different chambers. The amino acids isoleucine, leucine, and valine were particularly concentrated, whereas the concentration of glycine, asparagine, and serine was only slightly increased. Interestingly, in such chamber networks, both the thermophoretically strong species can be enriched over the weak species and vice versa, while at reduced absolute concentrations in the latter case. For example, glycine in the rear parts of the network will mainly be found in the upper chambers, as all species with strong thermophoresis have already been shuffled to the lower chambers by their effective accumulation. Enrichments of up to 2 orders of magnitude were also found for nucleotides of different phosphorylation states (regioisomers) and their nucleosides and bases or mixtures of nucleotide precursors.

Due to the strong enrichment of scarce phosphorylation reagents such as TMP, thermogravitational accumulation could thus have triggered its reaction with spatially separated prebiotic building blocks, which has been successfully demonstrated in a single heat flow chamber for a glycine dimerization reaction.<sup>[40]</sup> Numerically, an increase in the reaction yield of approx. 5 orders of magnitude up to several percent could be shown for this reaction in a system of 20 x 20 randomly connected chambers and an applied Temperature difference of  $\Delta T = 10K$ , exemplifying the benefits for prebiotic chemistry. Here, the reaction was driven by a local increase in TMP concentration due to its comparably high Soret coefficient ( $S_T \sim 7.5 \cdot 10^{-3} 1/K$ ) from initially 1  $\mu M$  to 10 mM within some chambers of the network, whereby the concentration boost would increase exponentially by further enlarging the overall system.<sup>[40]</sup> As TMP concentrations must have been extremely low due to the already small amounts of phosphorous (~100 ppm<sup>[198]</sup>) on the early Earth, such a selection mechanism would effectively utilize local TMP sources, e.g., in the vicinity of volcanoes.<sup>[199]</sup>

Such network systems could also provide a huge number of different reaction conditions simultaneously due to their volumetric scaling, which significantly increases the probability of finding the optimal initial composition for a specific prebiotic reaction. Constituting an open system, the network requires a constant flow of heat as well as a continuous feeding flow from outside. Without the former, there would be no local concentration differences, and all chambers would have identical compound compositions, whereas, without the latter, all chambers would only be diffusively coupled to each other and would exhibit very similar concentration profiles as in a single isolated chamber. Due to the constant slow geothermal flow, a continuous mixing process is thus simultaneously enabled in

each chamber by flows from previous chambers converging there. Remarkably, it could also be shown that the enrichment process works even with small temperature differences and can still take place effectively in natural systems due to the amplifying effect of their large size.

If evolving processes could thus develop slowly in individual chambers, the upstream synthesis of the required building blocks would ensure a sufficient and stable supply. The thermophoretic enrichment in connected, thin compartments could not only be an advantageous effect for prebiotic chemistry proposed in hydrothermal systems,<sup>[200,201]</sup> e.g., by enriching its products, but could also supply surfaces near ponds with starting materials that can react further there with the help of UV light.<sup>[10,202]</sup>

## Outlook

Much of the potential of geologically plausible networks of heat flow chambers is yet to be explored. One interesting application for such enrichment systems is its ability to select phosphorous-rich species in aqueous media. While said TMP-driven reactions profit considerably from thermogravitational enrichment, also mono-phosphorylated species show a relatively strong thermophoresis compared to their non-phosphorylated counterparts.<sup>[40]</sup> This could help with the solution of the so-called phosphate problem.<sup>[62,203]</sup> Phosphorous was presumably only available in small quantities on the early Earth and was not locally concentrated and maintained by modern life as it is today.<sup>[62]</sup> The phosphate present was probably mainly chelated with  $Ca^{2+}$  in the form of apatite, which is only effectively soluble in acidic conditions up to around pH 3 and is therefore inaccessible to the prebiotic chemistry often found in neutral or alkaline conditions. However, since the phosphate group is a central component for the function of (ribo-)oligonucleotides, phospholipids, and also protometabolic components,<sup>[204]</sup> the question arises as to how the small amount of phosphate present or bound could be utilized for phosphate-related prebiotic chemistry that often requires high millimolar concentrations of dissolved orthophosphate.<sup>[205,206]</sup>

Due to its importance, several approaches to the phosphate problem have been studied in detail. One possibility for prebiotic chemistry is the use of reduced phosphorous in the form of phosphites, which occurs in schreibersite supplied by iron meteorites.<sup>[207]</sup> In contrast to apatite, schreibersite is easily soluble in water and could therefore induce nucleoside phosphorylation at pH 9<sup>[208]</sup> or the production of amidophosphates<sup>[209]</sup> and trimetaphosphates.<sup>[63]</sup> Nucleoside phosphorylation was also demonstrated directly on apatite by using ammonium oxalate as a chelating agent for calcium, thus increasing the solubility of orthophosphates.<sup>[210]</sup> Carbonate lakes were identified as a very promising system in which up to molal concentrations of free phosphate can be found as calcium carbonate precipitates, preventing the formation of apatite.<sup>[211]</sup> Heat flows through thin cracks could drive an interesting, purely physical process here by separating calcium and phosphate ions through thermophoresis. The Seebeck effect from heat-

flow-driven charge separation has already been investigated experimentally for various ion pairs<sup>[44]</sup> and would lead here to a corresponding pH gradient, maintaining local charge neutrality.<sup>[41,80]</sup> The phosphate solubilized in this way could also be used for prebiotic reactions at neutral or alkaline pH. In the crack network system discussed above, phosphorylation reactions could therefore be triggered with the released phosphate, e.g., at gas-water interfaces, or generate different pH conditions as drivers of local pH gradients due to the different phosphate enrichments in each chamber.

This prospect is just one possible experimental model system that is waiting to be carried out. Only when it is shown how more complex prebiotic reaction pathways and networks can be driven with the help of such heat flow chamber systems can the potential for prebiotic chemistry be clearly assessed. Could different reaction pathways be implemented simultaneously in the different chambers due to the heat flow-driven differences in initial reactant compositions? Can RNA oligomers also be formed from non-activated nucleotides in such settings, e.g., with the help of TMP, and what sequence space would they occupy? Finally, it becomes clear that the enrichment from complex mixtures ultimately depends on how different the respective thermophoretic properties of the solutes are. Thermogravitational accumulation is also a slow effect whose coupling to prebiotic reactions also depends on their reaction rates.<sup>[41,42]</sup> Further investigation is required here for the case of mixed timescales, i.e., for slow reactions, which take place at a similar speed to thermophoresis-driven enrichment. Heat-flow-driven systems of interconnected chambers thus represent a promising model system for geological systems on the early Earth, the experimental exploration of which is only just beginning. Intensive interdisciplinary collaborations, more compact and mobile experimental setups that can accommodate more extensive chamber systems are the next step to exploring its full potential for prebiotic chemistry. Last but not least, the combination of heat flow-driven selection mechanisms with other selective physical processes, such as the interaction with the surrounding geomaterial, will be of high interest, leading to a more complete understanding of the complex non-equilibrium effects that might have played a crucial role in the origins of life.

## Author Contributions

Writing: CBM

## Acknowledgements

I thank Thomas Matreux, Saroj Rout, and Sreekar Wunnava for their comments on the manuscript. This work was funded by the Volkswagen Initiative 'Life? – A Fresh Scientific Approach to the Basic Principles of Life' (C.B.M.) and by the Deutsche Forschungsgemeinschaft (DFG, German Research Foundation) under Project-ID 364653263 – TRR 235 (C.B.M.) and Project-ID 521256690 – TRR 392 (C.B.M.). This work was supported by the

Center for Nanoscience Munich (CeNS). Open Access funding enabled and organized by Projekt DEAL.

## Conflict of Interests

No competing interests exist.

**Keywords:** Origin of Life · Non-equilibria · heat-flows · prebiotic chemistry · biophysics

- [1] B. H. Patel, C. Percivalle, D. J. Ritson, C. D. Duffy, J. D. Sutherland, *Nat. Chem.* **2015**, *7*, 301–307.
- [2] N. Lauber, C. Flamm, K. Ruiz-Mirazo, *BioEssays* **2021**, *43*, e2100103.
- [3] R. Pascal, I. A. Chen, *Nat. Chem.* **2019**, *11*, 763–764.
- [4] S. Otto, *Acc. Chem. Res.* **2022**, *55*, 145–155.
- [5] W. Huck, M. Baltussen, T. De Jong, Q. Duez, W. Robinson, *Nature* **2024**, *631*, 549–555.
- [6] W. T. S. Huck, A. Pogodaev, L. Fernandez-Rigueiro, M. Jakstaite, M. Hollander, *Angew. Chem. Int. Ed.* **2019**, *58*, 14539–14543.
- [7] W. E. Robinson, E. Daines, P. Van Duppen, T. De Jong, W. T. S. Huck, *Nat. Chem.* **2022**, *14*, 623–631.
- [8] A. Pross, *Curr. Org. Chem.* **2013**, *17*, 1702–1703.
- [9] R. M. Garner, A. T. Molines, J. A. Theriot, F. Chang, *Biophys. J.* **2023**, *122*, 767–783.
- [10] M. W. Powner, B. Gerland, J. D. Sutherland, *Nature* **2009**, *459*, 239–242.
- [11] H. M. McBride, M. Neuspiel, S. Wasiak, *Curr. Biol.* **2006**, *16*, R551–R560.
- [12] A. Bashan, A. Yonath, *Trends Microbiol.* **2008**, *16*, 326–335.
- [13] T. Mignot, J. W. Shaevitz, *Curr. Opin. Microbiol.* **2008**, *11*, 580–585.
- [14] G. B. West, J. H. Brown, B. J. Enquist, *Science* **1997**, *276*, 122–126.
- [15] C. Battle, C. P. Broedersz, N. Fakhri, V. F. Geyer, J. Howard, C. F. Schmidt, F. C. MacKintosh, *Science* **2016**, *352*, 604–607.
- [16] T. Okada, A. Mochizuki, *Phys. Rev. Lett.* **2016**, *117*, 048101.
- [17] J. C. Xavier, W. Hordijk, S. Kauffman, M. Steel, W. F. Martin, *Proceedings of the Royal Society B-Biological Sciences* **2020**, *287*, 1922.
- [18] E. Karzbrun, A. M. Tayar, V. Noireaux, R. H. Bar-Ziv, *Science* **2014**, *345*, 829–832.
- [19] P. Glock, F. Brauns, J. Halatek, E. Frey, P. Schwillie, *eLife* **2019**, *8*, e48646.
- [20] S. A. Benner, E. A. Bell, E. Biondi, R. Brassler, T. Carell, H.-J. Kim, S. J. Mojzsis, A. Omran, M. A. Pasek, D. Trail, *ChemSystemsChem* **2020**, *2*, e1900035.
- [21] A. Ianeselli, A. Salditt, C. Mast, B. Ercolano, C. L. Kufner, B. Scheu, D. Braun, *Nat Rev Phys* **2023**, *5*, 185–195.
- [22] C. H. Lineweaver, C. A. Egan, *Physics of Life Reviews* **2008**, *5*, 225–242.
- [23] E. A. Frank, B. S. Meyer, S. J. Mojzsis, *Icarus* **2014**, *243*, 274–286.
- [24] W. F. McDonough, O. Šrámek, S. A. Wipperfurth, *Geochem. Geophys. Geosyst.* **2020**, *21*, e2019GC008865.
- [25] R. Barnes, B. Jackson, R. Greenberg, S. N. Raymond, *ApJ* **2009**, *700*, L30–L33.
- [26] F. Pirajno, *Hydrothermal Processes and Mineral Systems*, Springer, Dordrecht, **2010**, pp. 581–632.
- [27] J. van Otterloo, R. A. F. Cas, C. R. Scutter, *Earth-Sci. Rev.* **2015**, *151*, 79–116.
- [28] M. Colombier, B. Scheu, U. Kueppers, S. J. Cronin, S. B. Mueller, K.-U. Hess, F. B. Wadsworth, M. Tost, K. J. Dobson, B. Ruthensteiner, D. B. Dingwell, *Geology* **2019**, *47*, 179–182.
- [29] L. Bai, D. R. Baker, R. J. Hill, *J. Geophys. Res.* **2010**, *115*, B07201.
- [30] D. S. Kelley, J. A. Karson, G. L. Früh-Green, D. R. Yoerger, T. M. Shank, D. A. Butterfield, J. M. Hayes, M. O. Schrenk, E. J. Olson, G. Proskurowski, M. Jakuba, A. Bradley, B. Larson, K. Ludwig, D. Glickson, K. Buckman, A. S. Bradley, W. J. Brazelton, K. Roe, M. J. Elend, A. Delacour, S. M. Bernasconi, M. D. Lilley, J. A. Baross, R. E. Summons, S. P. Sylva, *Science* **2005**, *307*, 1428–1434.
- [31] N. G. Holm, C. Oze, O. Mousis, J. H. Waite, A. Guilbert-Lepoutre, *Astrobiology* **2015**, *15*, 587–600.
- [32] B. Herschy, A. Whicher, E. Camprubi, C. Watson, L. Dartnell, J. Ward, J. R. G. Evans, N. Lane, *J. Mol. Evol.* **2014**, *79*, 213–227.
- [33] J. F. Kasting, R. Kopparapu, R. M. Ramirez, C. E. Harman, *Proc. Natl. Acad. Sci. USA* **2014**, *111*, 12641–12646.
- [34] F. J. Martín-Torres, M.-P. Zorzano, P. Valentín-Serrano, A.-M. Harri, M. Genzer, O. Kempainen, E. G. Rivera-Valentin, I. Jun, J. Wray, M.

- Bo Madsen, W. Goetz, A. S. McEwen, C. Hardgrove, N. Renno, V. F. Chevrier, M. Mischna, R. Navarro-González, J. Martínez-Frías, P. Conrad, T. McConnochie, C. Cockell, G. Berger, A. R. Vasavada, D. Sumner, D. Vaniman, *Nature Geosci* **2015**, *8*, 357–361.
- [35] C. Chyba, C. Sagan, *Nature* **1992**, *355*, 125–132.
- [36] Y. Takeuchi, Y. Furukawa, T. Kobayashi, T. Sekine, N. Terada, T. Kakegawa, *Sci. Rep.* **2020**, *10*, 9220.
- [37] K. Kadoya, N. Matsunaga, A. Nagashima, *J. Phys. Chem. Ref. Data* **1985**, *14*, 947–970.
- [38] M. L. V. Ramires, C. A. Nieto De Castro, Y. Nagasaka, A. Nagashima, M. J. Assael, W. A. Wakeham, *J. Phys. Chem. Ref. Data* **1995**, *24*, 1377–1381.
- [39] L. Keil, M. Hartmann, S. Lanzmich, D. Braun, *Physical chemistry chemical physics: PCCP* **2016**, *18*, 20153–20159.
- [40] T. Matreux, P. Aikkila, B. Scheu, D. Braun, C. B. Mast, *Nature* **2024**, *628*, 110–116.
- [41] T. Matreux, B. Altaner, J. Raith, D. Braun, C. B. Mast, U. Gerland, *Commun. Phys.* **2023**, *6*, 14.
- [42] C. B. Mast, S. Schink, U. Gerland, D. Braun, *Proc. Natl. Acad. Sci. USA* **2013**, *110*, 8030–8035.
- [43] T. Matreux, K. Le Vay, A. Schmid, P. Aikkila, L. Belohlavek, A. Z. Çalişkanoglu, E. Salibi, A. Kühnlein, C. Springsklee, B. Scheu, D. B. Dingwell, D. Braun, H. Mutschler, C. B. Mast, *Nat. Chem.* **2021**, *13*, 1038–1045.
- [44] M. Reichl, M. Herzog, A. Götz, D. Braun, *Phys. Rev. Lett.* **2014**, *112*, 198101.
- [45] S. Duhr, D. Braun, *Phys. Rev. Lett.* **2006**, *96*, 168301.
- [46] D. B. Mayer, T. Franosch, C. Mast, D. Braun, *Phys. Rev. Lett.* **2023**, *130*, 168202.
- [47] S. Wiegand, *J. Phys. Condens. Matter* **2004**, *16*, R357.
- [48] Z. Wang, H. Kriegs, S. Wiegand, *J. Phys. Chem. B* **2012**, *116*, 7463–7469.
- [49] P. Reineck, C. J. Wienken, D. Braun, *Electrophoresis* **2010**, *31*, 279–286.
- [50] S. Duhr, S. Arduini, D. Braun, *The European Physical Journal E* **2004**, *15*, 277–286.
- [51] D. Niether, D. Afanasenkau, J. K. G. Dhont, S. Wiegand, *Proc. Natl. Acad. Sci. USA* **2016**, *113*, 4272–4277.
- [52] A. Würger, *Comptes Rendus Mécanique* **2013**, *341*, 438–448.
- [53] S. Fayolle, T. Bickel, A. Würger, *Phys. Rev. E* **2008**, *77*, 041404.
- [54] S. Duhr, D. Braun, *Proc. Natl. Acad. Sci. USA* **2006**, *103*, 19678–19682.
- [55] A. Parola, R. Piazza, *Eur. Phys. J. E* **2004**, *15*, 255–263.
- [56] J. K. G. Dhont, *J. Chem. Phys.* **2004**, *120*, 1632–1641.
- [57] J. Burelbach, D. Frenkel, I. Pagonabarraga, E. Eiser, *The European physical journal. E, Soft matter* **2018**, *41*, 7.
- [58] A. Diaz-Marquez, G. Stirnemann, *J. Chem. Phys.* **2021**, *155*, 174503.
- [59] N. Takeyama, K. Nakashima, *J. Solution Chem.* **1988**, *17*, 305–325.
- [60] C. J. Wienken, P. Baaske, U. Rothbauer, D. Braun, S. Duhr, *Nat. Commun.* **2010**, *1*, 100.
- [61] K. Le Vay, E. Salibi, E. Y. Song, H. Mutschler, *Chem. Asian J.* **2020**, *15*, 214–230.
- [62] C. R. Walton, S. Ewens, J. D. Coates, R. E. Blake, N. J. Planavsky, C. Reinhard, P. Ju, J. Hao, M. A. Pasek, *Nat. Geosci.* **2023**, *16*, 399–409.
- [63] R. Osterberg, L. E. Orgel, *J. Mol. Evol.* **1972**, *1*, 241–248.
- [64] H. Sugahara, K. Mimura, *Geochem. J.* **2014**, *48*, 51–62.
- [65] J. N. Agar, J. C. R. Turner, *J. Phys. Chem.* **1960**, *64*, 1000–1003.
- [66] N. Lee, S. Wiegand, *Entropy (Basel)* **2020**, *22*, 950.
- [67] M. Hartung, W. Köhler, *Rev. Sci. Instrum.* **2007**, *78*, 084901.
- [68] Y. Zhao, C. Zhao, J. He, Y. Zhou, C. Yang, *Soft Matter* **2013**, *9*, 7726.
- [69] W. Köhler, S. Wiegand, *Thermal Nonequilibrium Phenomena in Fluid Mixtures*, Springer, Berlin, New York, **2002**, pp. 189–210.
- [70] S. Wiegand, H. Ning, H. Kriegs, *J. Phys. Chem. B* **2007**, *111*, 14169–14174.
- [71] P. Naumann, A. Martin, H. Kriegs, M. Larrañaga, M. M. Bou-Ali, S. Wiegand, *J. Phys. Chem. B* **2012**, *116*, 13889–13897.
- [72] E. Lapeira, A. Mialdun, V. Yasnou, P. Aristimuño, V. Shevtsova, M. M. Bou-Ali, *Microgravity Sci. Technol.* **2018**, *30*, 635–641.
- [73] C. J. Wienken, P. Baaske, U. Rothbauer, D. Braun, S. Duhr, *Nat. Commun.* **2010**, *1*, 100.
- [74] M. Jerabek-Willemsen, T. André, R. Wanner, H. M. Roth, S. Duhr, P. Baaske, D. Breitsprecher, *J. Mol. Struct.* **2014**, *1077*, 101–113.
- [75] M. Reichl, M. Herzog, F. Greiss, M. Wolff, D. Braun, *Phys. Rev. E* **2015**, *91*, 062709.
- [76] K. Clusius, G. Dickel, *Die Naturwissenschaften* **1938**, *26*, 546.
- [77] P. Debye, *Annalen der Physik* **1939**, *428*, 284–294.
- [78] O. Ecenarro, J. A. Madariaga, J. Navarro, C. M. Santamaria, J. A. Carrión, J. M. Savirón, *Sep. Sci. Technol.* **1989**, *24*, 555–568.
- [79] P. Blanco, P. Polyakov, M. M. Bou-Ali, S. Wiegand, *J. Phys. Chem. B* **2008**, *112*, 8340–8345.
- [80] L. M. R. Keil, F. M. Möller, M. Kieß, P. W. Kudella, C. B. Mast, *Nat. Commun.* **2017**, *8*, 1897.
- [81] D. Luo, C. Zhao, G. Xue, Z. Cao, A. Oztekin, X. Cheng, *RSC Adv.* **2022**, *12*, 4263–4275.
- [82] A. Martin-Mayor, M. M. Bou-Ali, M. Aginagalde, P. Urteaga, *Int. J. Therm. Sci.* **2018**, *124*, 279–287.
- [83] A. V. Dass, S. Wunnavu, J. Langlais, B. von der Esch, M. Krusche, L. Ufer, N. Chrisam, R. C. A. Dubini, F. Gartner, S. Angerpointner, C. F. Dirscherl, P. Rovó, C. B. Mast, J. E. Sponer, C. Ochsenfeld, E. Frey, D. Braun, *ChemSystemsChem* **2023**, *5*, e202200026. DOI 10.1002/syst.202200026.
- [84] P. Baaske, F. M. Weinert, S. Duhr, K. H. Lemke, M. J. Russell, D. Braun, *Proc. Natl. Acad. Sci. USA* **2007**, *104*, 9346–9351.
- [85] E. V. Koonin, *Proc. Natl. Acad. Sci. USA* **2007**, *104*, 9105–9106.
- [86] C. F. Dirscherl, A. Ianeselli, D. Tetiker, T. Matreux, R. M. Queener, C. B. Mast, D. Braun, *Phys. Chem. Phys.* **2023**, *25*, 3375–3386.
- [87] T. Saiki, N. Ono, S. Matsumoto, S. Watanabe, *Int. J. Heat Mass Transfer* **2020**, *163*, 120394.
- [88] R. K. Prabhudesai, J. E. Powers, *Ann. N. Y. Acad. Sci.* **1966**, *137*, 83–102.
- [89] M. Chen, L. Zheng, B. Santra, H.-Y. Ko, R. A. DiStasio Jr, M. L. Klein, R. Car, X. Wu, *Nature Chem* **2018**, *10*, 413–419.
- [90] P. Adamski, M. Eleveld, A. Sood, A. Kun, A. Szilagy, T. Czarán, E. Szathmáry, S. Otto, *Nat. Chem. Rev.* **2020**, *4*, 386–403.
- [91] S. Islam, M. W. Powner, *Chem* **2017**, *2*, 470–501.
- [92] P. G. Higgs, N. Lehman, *Nat. Rev. Genet.* **2015**, *16*, 7–17.
- [93] G. F. Joyce, in *Chemistry Challenges of the 21st Century*, WORLD SCIENTIFIC, **2023**, pp. 433–439.
- [94] W. Gilbert, *Nature* **1986**, *319*, 618.
- [95] G. F. Joyce, *Nature* **2002**, *418*, 214–221.
- [96] T. R. Cech, *Gene* **1993**, *135*, 33–36.
- [97] K. Adamala, J. W. Szostak, *Nat. Chem.* **2013**, *5*, 495–501.
- [98] F. Müller, L. Escobar, F. Xu, E. Węgrzyn, M. Nainyć, T. Amatov, C.-Y. Chan, A. Pichler, T. Carell, *Nature* **2022**, *605*, 279–284.
- [99] K. F. Tjhung, M. N. Shokhirev, D. P. Horning, G. F. Joyce, *Proc. Natl. Acad. Sci. USA* **2020**, *117*, 2906–2913.
- [100] R. Cojocar, P. J. Unrau, *Science* **2021**, *371*, 1225–1232.
- [101] R. Green, J. W. Szostak, *Science* **1992**, *258*, 1910–1915.
- [102] N. Paul, G. F. Joyce, *Proc. Natl. Acad. Sci. USA* **2002**, *99*, 12733–12740.
- [103] D. P. Bartel, J. W. Szostak, *Science* **1993**, *261*, 1411–1418.
- [104] J. Attwater, A. Wochner, P. Holliger, *Nat. Chem.* **2013**, *5*, 1011–1018.
- [105] G. A. L. Bare, G. F. Joyce, *J. Am. Chem. Soc.* **2021**, *143*, 19160–19166.
- [106] D. P. Horning, S. Bala, J. C. Chaput, G. F. Joyce, *ACS Synth. Biol.* **2019**, *8*, 955–961. DOI 10.1021/acssynbio.9b00044.
- [107] M. Eigen, *Die Naturwissenschaften* **1971**, *58*, 465–523.
- [108] T. Walton, W. Zhang, L. Li, C. P. Tam, J. W. Szostak, *Angew. Chem. Int. Ed.* **2019**, *58*, 10812–10819. DOI 10.1002/anie.201902050.
- [109] S. R. Vogel, C. Deck, C. Richert, *Chem. Commun.* **2005**, *39*, 4922–4924.
- [110] L. Zhou, D. K. O’Flaherty, J. W. Szostak, *Angew. Chem. Int. Ed.* **2020**, *59*, 15682–15687.
- [111] A. Calaça Serrão, S. Wunnavu, A. Vicholous Dass, L. Ufer, P. Schwintek, C. B. Mast, D. Braun, *J. Am. Chem. Soc.* **2024**, *146*, 8887–8894.
- [112] S. Rajamani, J. K. Ichida, T. Antal, D. A. Treco, K. Leu, M. A. Nowak, J. W. Szostak, I. A. Chen, *J. Am. Chem. Soc.* **2010**, *132*, 5880–5885.
- [113] K. Leu, E. Kervio, B. Obermayer, R. M. Turk-MacLeod, C. Yuan, J.-M. Luevano, E. Chen, U. Gerland, C. Richert, I. A. Chen, *J. Am. Chem. Soc.* **2013**, *135*, 354–366.
- [114] G. Von Kiedrowski, in *Bioorganic Chemistry Frontiers* (Eds.: H. Dugas, F. P. Schmidtchen), Springer Berlin Heidelberg, Berlin, Heidelberg, **1993**, pp. 113–146.
- [115] E. Szathmáry, I. Gladkih, *J. Theor. Biol.* **1989**, *138*, 55–58.
- [116] A. S. Tupper, P. G. Higgs, *J. Theor. Biol.* **2021**, *527*, 110822.
- [117] Y. Li, R. R. Breaker, *J. Am. Chem. Soc.* **1999**, *121*, 5364–5372.
- [118] C. A. Heid, J. Stevens, K. J. Livak, P. M. Williams, *Genome Res.* **1996**, *6*, 986–994.
- [119] C. Deck, M. Jauker, C. Richert, *Nat. Chem.* **2011**, *3*, 603–608.
- [120] K. Adamala, J. W. Szostak, *Science* **2013**, *342*, 1098–1100.
- [121] T. Hassenkam, D. Deamer, *Sci. Rep.* **2022**, *12*, 10098.
- [122] S. Dagar, S. Sarkar, S. Rajamani, *Orig. Life Evol. Biosph.* **2023**, *53*, 43–60. DOI 10.1007/s11084-023-09636-z.
- [123] H. Mutschler, A. Wochner, P. Holliger, *Nat. Chem.* **2015**, *7*, 502–508.
- [124] P. Śulc, T. E. Ouldrige, F. Romano, J. P. K. Doye, A. A. Louis, *Biophys. J.* **2015**, *108*, 1238–1247.
- [125] L. Zhou, S. Kim, K. H. Ho, D. K. O’Flaherty, C. Giurgiu, T. H. Wright, J. W. Szostak, *eLife* **2019**, *8*, e51888. DOI 10.7554/eLife.51888.

- [126] E. L. Kristoffersen, M. Burman, A. Noy, P. Holliger, *eLife* **2022**, *11*, 25.
- [127] L. J. Zhou, D. Ding, J. W. Szostak, *RNA* **2021**, *27*, 1–11.
- [128] D. Ding, L. Zhou, S. Mittal, J. W. Szostak, *J. Am. Chem. Soc.* **2023**, *145*, 7504–7515. jacs.3c00612.
- [129] R. Lathé, *Icarus* **2004**, *168*, 18–22.
- [130] T. Ebisuzaki, S. Maruyama, *Geoscience Frontiers* **2017**, *8*, 275–298.
- [131] J. W. Szostak, *J. Syst. Chem.* **2012**, *3*, 2.
- [132] D. P. Horning, G. F. Joyce, *Proc. Natl. Acad. Sci. USA* **2016**, *113*, 9786–9791.
- [133] A. Salditt, L. M. R. Keil, D. P. Horning, C. B. Mast, G. F. Joyce, D. Braun, *Phys. Rev. Lett.* **2020**, *125*, 048104.
- [134] C. B. Mast, D. Braun, *Phys. Rev. Lett.* **2010**, *104*, 188102.
- [135] M. Kreyising, L. Keil, S. Lanzmich, D. Braun, *Nat. Chem.* **2015**, *7*, 203–208.
- [136] D. R. Mills, R. L. Peterson, S. Spiegelman, *Proc. Natl. Acad. Sci. USA* **1967**, *58*, 217–224.
- [137] G. Leveau, D. Pfeffer, B. Altaner, E. Kervio, F. Welsch, U. Gerland, C. Richert, *Angew. Chem. Int. Ed.* **2022**, *61*, e202203067.
- [138] Z.-J. Tan, S.-J. Chen, *Biophys. J.* **2007**, *92*, 3615–3632.
- [139] A. Mariani, C. Bonfio, C. M. Johnson, J. D. Sutherland, *Biochemistry* **2018**, *57*, 6382–6386. DOI 10.1021/acs.biochem.8b01080.
- [140] A. Ianeselli, C. B. Mast, D. Braun, *Angew. Chem.* **2019**, *131*, 13289–13294.
- [141] A. Ianeselli, M. Atienza, P. W. Kudella, U. Gerland, C. B. Mast, D. Braun, *Nat. Phys.* **2022**, *18*, 579–585.
- [142] A. Salditt, L. Karr, E. Salibi, K. Le Vay, D. Braun, H. Mutschler, *Nat. Commun.* **2023**, *14*, 1495.
- [143] C. Bonfio, D. A. Russell, N. J. Green, A. Mariani, J. D. Sutherland, *Chem. Sci.* **2020**, *11*, 10688–10697.
- [144] I. Budin, R. J. Bruckner, J. W. Szostak, *J. Am. Chem. Soc.* **2009**, *131*, 9628–9629.
- [145] F. Chizzolini, L. F. M. Passalacqua, M. Oumais, A. I. Dingilian, J. W. Szostak, A. Lupták, *J. Am. Chem. Soc.* **2020**, *142*, 1941–1951.
- [146] N. A. Hawbaker, D. G. Blackmond, *Nat. Chem.* **2019**, *11*, 957–962.
- [147] M. Deng, J. Yu, D. G. Blackmond, *Nature* **2024**, *626*, 1019–1024.
- [148] G. Storch, O. Trapp, *Nat. Chem.* **2016**, *9*, 179–187.
- [149] M. P. Robertson, G. F. Joyce, *Cold Spring Harbor Perspect. Biol.* **2012**, *4*, a003608. DOI 10.1101/cshperspect.a003608.
- [150] S. A. Benner, *Origins Life Evol. Biospheres* **2014**, *44*, 339–343.
- [151] K. Zhang, J. Hodge, A. Chatterjee, T. S. Moon, K. M. Parker, *Environ. Sci. Technol.* **2021**, *55*, 8045–8053.
- [152] M. Morasch, D. Braun, C. B. Mast, *Angew. Chem. Int. Ed.* **2016**, *55*, 6676–6679.
- [153] S. Matsumura, A. Kun, M. Ryckelynck, F. Coldren, A. Szilagyi, F. Jossinet, C. Rick, P. Nghe, E. Szathmary, A. D. Griffiths, *Science* **2016**, *354*, 1293–1296.
- [154] R. Mizuuchi, A. Blokhuis, L. Vincent, P. Nghe, N. Lehman, D. Baum, *Chem. Commun.* **2019**, *55*, 2090–2093.
- [155] R. Saha, W.-L. Kao, B. Malady, X. Heng, I. A. Chen, *Biophys. J.* **2023**, *123*, 451–463. S0006349523006872.
- [156] G. Bartolucci, A. Calça Serrão, P. Schwintek, A. Kühnlein, Y. Rana, P. Janto, D. Hofer, C. B. Mast, D. Braun, C. A. Weber, *Proc. Natl. Acad. Sci. USA* **2023**, *120*, e2218876120.
- [157] M. P. Friedmann, V. Torbeev, V. Zelenay, A. Sobol, J. Greenwald, R. Riek, *PLoS One* **2015**, *10*, 16.
- [158] J. Greenwald, W. Kwiatkowski, R. Riek, *J. Mol. Biol.* **2018**, *430*, 3735–3750.
- [159] K. Le Vay, E. Y. Song, B. Ghosh, T.-Y. D. Tang, H. Mutschler, *Angew. Chem.* **2021**, *133*, 26300–26308.
- [160] A. D. Sloodbeek, M. H. I. Van Haren, I. B. A. Smokers, E. Spruijt, *Chem. Commun.* **2022**, *58*, 11183–11200.
- [161] D. Wollny, B. Vernet, J. Wang, M. Hondele, A. Safrastyan, F. Aron, J. Micheel, Z. He, A. Hyman, K. Weis, J. G. Camp, T.-Y. D. Tang, B. Treutlein, *Nat. Commun.* **2022**, *13*, 2626.
- [162] K. K. Le Vay, E. Salibi, B. Ghosh, T. D. Tang, H. Mutschler, *eLife* **2023**, *12*, e83543.
- [163] M. D'Abramo, C. L. Castellazzi, M. Orozco, A. Amadei, *J. Phys. Chem. B* **2013**, *117*, 8697–8704.
- [164] R. Saha, I. Chen, *Chembiochem: a European journal of chemical biology* **2019**, *20*, 2609–2617.
- [165] C. L. Kufner, S. Krebs, M. Fischaleck, J. Philippou-Massier, H. Blum, D. B. Bucher, D. Braun, W. Zinth, C. B. Mast, *Sci. Rep.* **2023**, *13*, 2638.
- [166] H. S. Zaher, P. J. Unrau, *RNA* **2007**, *13*, 1017–1026.
- [167] S. Toyabe, *Phys. Rev. X* **2019**, *9*, 011056. DOI 10.1103/PhysRevX.9.011056.
- [168] P. W. Kudella, A. V. Tkachenko, A. Salditt, S. Maslov, D. Braun, *Proc. Natl. Acad. Sci. USA* **2021**, *118*, e2018830118.
- [169] D. G. Blackmond, *Cold Spring Harbor Perspect. Biol.* **2019**, *11*, a032540. DOI 10.1101/cshperspect.a032540.
- [170] Q. Sallembien, L. Bouteiller, J. Crassous, M. Raynal, *Chem. Soc. Rev.* **2022**, *51*, 3436–3476.
- [171] K. Soai, T. Shibata, H. Morioka, K. Choji, *Nature* **1995**, *378*, 767–768.
- [172] J. E. Hein, E. Tse, D. G. Blackmond, *Nat. Chem.* **2011**, *3*, 704–706.
- [173] S. F. Ozturk, Z. Liu, J. D. Sutherland, D. D. Sasselov, *Sci. Adv.* **2023**, *9*, eadg8274.
- [174] S. F. Ozturk, D. K. Bhowmick, Y. Kapon, Y. Sang, A. Kumar, Y. Paltiel, R. Naaman, D. D. Sasselov, *Nat. Commun.* **2023**, *14*, 6351.
- [175] S. Yang, Y. Geiger, M. Geerts, M. J. Eleveld, A. Kiani, S. Otto, *J. Am. Chem. Soc.* **2023**, *145*, 16889–16898.
- [176] G. Laurent, D. Lacoste, P. Gaspard, *Proc. Natl. Acad. Sci. USA* **2021**, *118*, e2012741118.
- [177] M. Morasch, J. Liu, C. F. Dirscherl, A. Ianeselli, A. Kühnlein, K. Le Vay, P. Schwintek, S. Islam, M. K. Corpinot, B. Scheu, D. B. Dingwell, P. Schwiller, H. Mutschler, M. W. Powner, C. B. Mast, D. Braun, *Nat. Chem.* **2019**, *11*, 779–788.
- [178] C. Anastasi, M. A. Crowe, M. W. Powner, J. D. Sutherland, *Angew. Chem.* **2006**, *118*, 6322–6325.
- [179] K. Hoehlig, L. Bethge, S. Klusmann, *PLoS One* **2015**, *10*, e0115328.
- [180] J. Krissansen-Totton, G. N. Arney, D. C. Catling, *Proc. Natl. Acad. Sci. USA* **2018**, *115*, 4105–4110.
- [181] S. L. Miller, *Science* **1953**, *117*, 528–529.
- [182] S. A. Benner, H. J. Kim, M. A. Carrigan, *Acc. Chem. Res.* **2012**, *45*, 2025–2034.
- [183] J. Yi, H. Kaur, W. Kazone, S. A. Rauscher, L. A. Gravillier, K. B. Muchowska, J. Moran, *Angew. Chem. Int. Ed.* **2022**, *61*, e202117211.
- [184] J. S. Teichert, F. M. Kruse, O. Trapp, *Angew. Chem. Int. Ed.* **2019**, *58*, 9944–9947.
- [185] T. P. Roche, D. M. Fialho, C. Menor-Salván, R. Krishnamurthy, G. B. Schuster, N. V. Hud, *Chem. Eur. J.* **2023**, *29*, e202203036.
- [186] D. J. Ritson, C. Battilocchio, S. V. Ley, J. D. Sutherland, *Nat. Commun.* **2018**, *9*, 1821.
- [187] S. Becker, J. Feldmann, S. Wiedemann, H. Okamura, C. Schneider, K. Iwan, A. Crisp, M. Rossa, T. Amatov, T. Carell, *Science* **2019**, *366*, 76–82.
- [188] F. Kruse, J. Teichert, O. Trapp, *Chemistry (Weinheim an der Bergstrasse, Germany)* **2020**, *26*, 14776–14790.
- [189] N. Kitadai, K. Nishiuchi, W. Takahagi, *Minerals* **2021**, *11*, 17.
- [190] M. Haas, S. Lamour, S. B. Christ, O. Trapp, *Communications Chemistry* **2020**, *3*, 140. DOI 10.1038/s42004-020-00387-w.
- [191] J. P. Ferris, G. Ertem, *Origins Life Evol. Biospheres* **1992**, *22*, 369–381.
- [192] P. Canavelli, S. Islam, M. W. Powner, *Nature* **2019**, *571*, 546–549.
- [193] M. Frenkel-Pinter, J. W. Haynes, M. C. A. S. Petrov, B. T. Burcar, R. Krishnamurthy, N. V. Hud, L. J. Leman, L. D. Williams, *Proc. Natl. Acad. Sci. USA* **2019**, *116*, 16338–16346.
- [194] T. D. Campbell, R. Febrian, J. T. McCarthy, H. E. Kleinschmidt, J. G. Forsythe, P. J. Bracher, *Nat. Commun.* **2019**, *10*, 4508.
- [195] M. Frenkel-Pinter, J. W. Haynes, A. M. Mohyeldin, M. C. A. B. Sargon, A. S. Petrov, R. Krishnamurthy, N. V. Hud, L. D. Williams, L. J. Leman, *Nat. Commun.* **2020**, *11*, 3137.
- [196] S. K. Rout, R. Cadalbert, N. Schröder, J. Wang, J. Zehnder, O. Gampp, T. Wiegand, P. Güntert, D. Klingler, C. Kreutz, A. Knörlein, J. Hall, J. Greenwald, R. Riek, *J. Am. Chem. Soc.* **2023**, *145*, 21915–21924.
- [197] A. V. Getling, *Rayleigh-Bénard Convection: Structures and Dynamics*, World Scientific, Singapore; River Edge, NJ, **1998**, pp. 59–119.
- [198] C. R. Walton, O. Shorttle, F. E. Jenner, H. M. Williams, J. Golden, S. M. Morrison, R. T. Downs, A. Zerkle, R. M. Hazen, M. Pasek, *Earth-Sci. Rev.* **2021**, *221*, 103806.
- [199] Y. Yamagata, H. Watanabe, M. Saitoh, T. Namba, *Nature* **1991**, *352*, 516–519.
- [200] M. J. Russell, *Acta Biotheor.* **2009**, *57*, 389–394.
- [201] M. Preiner, K. Igarashi, K. B. Muchowska, M. Yu, S. J. Varma, K. Kleinermanns, M. K. Nobu, Y. Kamagata, H. Tüysüz, J. Moran, W. F. Martin, *Nat. Ecol. Evol.* **2020**, *4*, 534–542.
- [202] S. Ranjan, C. L. Kufner, G. G. Lozano, Z. R. Todd, A. Haseki, D. D. Sasselov, *Astrobiology* **2022**, *22*, 242–262.
- [203] M. A. Pasek, *Proc. Natl. Acad. Sci. USA* **2008**, *105*, 853–858.
- [204] N. Nogal, J. Luis-Barrera, S. Vela-Gallego, F. Aguilar-Galindo, A. De La Escosura, *Org. Chem. Front.* **2024**, *11*, 1924–1932.
- [205] R. Lohrmann, L. E. Orgel, *Science* **1968**, *161*, 64–.
- [206] C. Ponnampereuma, R. Mack, *Science* **1965**, *148*, 1221–1223.
- [207] M. A. Pasek, *Geoscience Frontiers* **2017**, *8*, 329–335.

- [208] M. Gull, M. A. Mojica, F. M. Fernández, D. A. Gaul, T. M. Orlando, C. L. Liotta, M. A. Pasek, *Sci. Rep.* **2015**, *5*, 17198.
- [209] C. Gibard, I. B. Gorrell, E. I. Jiménez, T. P. Kee, M. A. Pasek, R. Krishnamurthy, *Angew. Chem. Int. Ed.* **2019**, *58*, 8151–8155.
- [210] A. W. Schwartz, *Biochimica et Biophysica Acta (BBA) - Nucleic Acids and Protein Synthesis* **1972**, *281*, 477–480.
- [211] J. D. Toner, D. C. Catling, *Proc. Natl. Acad. Sci. USA* **2020**, *117*, 883–888.

---

Manuscript received: April 30, 2024  
Version of record online: August 2, 2024

---